# Atmospheric contribution to cations cycling in highly weathered catchment, Guadeloupe (Lesser Antilles)

Celine Dessert, Clémentine Clergue, Alain Maurice Adolphe Antoine Rousteau, Olivier Crispi, Marc F Benedetti

# Atmospheric contribution to cations cycling in highly weathered catchment, Guadeloupe (Lesser Antilles)

Céline Dessert[1,a], Clémentine Clergue[1], Alain Rousteau[2], Olivier Crispi[1,b], Marc F. Benedetti[1]

[1]Université de Paris, Institut de physique du globe de Paris, CNRS, F-75005 Paris, France

[2]Laboratoire de biologie et de physiologie végétales, UMR EcoFoG, CNRS, Cirad, INRA, Université des Antilles, Université de Guyane, 97159 Pointe-à-Pitre, France

[a] corresponding author: E-mail address: dessert@ipgp.fr (Céline Dessert)

[b] present address: Laboratoire d'océanographie biologique, UMR 7621, Laboratoire Arago, BP 44, 66651 Banyuls-sur-Mer cedex, France

**Keywords:** Atmospheric deposit, Saharan dust, cation-nutrient recycling, Sr and Nd isotopes, Critical Zone.

**Abstract:**

The important fertilizing role of atmospheric dust, and particularly African dust, in tropical rainforests is increasingly recognized but still poorly quantified. To better evaluate dust input into the Caribbean basin, we sampled critical zone compartments of a small forested volcanic catchment in Guadeloupe (soils, parent rock, atmospheric dust, plants, soil solutions, stream and rain waters). The aims of this

study are to track sources of cation nutrients (Ca, Mg, K, Sr) developed on highly weathered soil in the rainforest of Guadeloupe, to quantify plant recycling of these nutrients, and to identify constraints on regolith development and its associated nutrient pool.

In the Quiock Creek catchment, a large isotopic range of $^{87}Sr/^{86}Sr$ and εNd values was observed despite the small scale of observation. Sr isotopic composition of the dissolved load varied from 0.7084 in rainfall to 0.7110 in soil solution, whereas it ranges between 0.7068 and 0.7153 for soil samples and between 0.7096 and 0.7102 for plants. The Nd isotopic composition varied between -8.39 in near-surface soil samples to 2.71 in deeper soil. All samples had an intermediate signature between that of the bedrock endmember ($^{87}Sr/^{86}Sr$=0.7038; εNd=4.8) and the atmospheric endmember (sea salt: $^{87}Sr/^{86}Sr$=0.7092 and Saharan dust: $^{87}Sr/^{86}Sr$=0.7187, εNd=-11.5).

The regolith was built on pyroclastic deposits, but, because of extreme leaching, the regolith has lost its original bedrock signature and inherited an exogenous atmospheric signature. Our results show that only the chemical weathering of the fresh near-surface minerals can provide nutrients to the ecosystem (first 30 cm). However, this dust weathering is too low to sustain the tropical forest ecosystem on its own. The cationic mass balance at the catchment scale, as well as the Sr isotopic signature, show that cation and Sr fluxes are of atmospheric origin only and that original bedrock no longer participates in nutrient cycles. The vegetation reflects the $^{87}Sr/^{86}Sr$ of the dissolved pool of atmospheric Sr.

At the soil-plant scale, the cation-nutrient fluxes provided by vegetation (litter fall + leaf excretion) are major compared to input and output fluxes. The annual Ca, K, Sr and Mg fluxes within the vegetation are, respectively, 31, 28, 20 and 3 times greater than the exported fluxes at the outlet of the basin. The residence time of nutrients in the vegetation is 16 years for K and close to 45 years for Sr, Ca and Mg. These results emphasize the highly efficient vegetative turnover that dominates the nutrient cycle in the Quiock Creek catchment.

This first characterization of biogeochemical cycles in the Guadeloupean rainforest suggests that the forest community of Quiock Creek is sustained by a small near-surface nutrient pool disconnected from

47 the deep volcanic bedrock. We also demonstrated that, even with efficient nutrient recycling, Saharan
48 dust plays a significant role in maintaining ecosystem productivity in Guadeloupe over long-time scales.

## 1. Introduction

The base cations calcium, potassium and magnesium, are nutrient elements essential for plant development as they are building blocks of tissues and chlorophyll and have a number of metabolic functions. They also play a major role in neutralizing soil acidity and maintaining biological activity. In ecosystems, base cations in soils and plants originate from in situ mineral weathering (*e.g.* Schlesinger, 1997). However, numerous studies have shown that, under specific circumstances, these elements can be provided by the atmosphere through precipitation or dust (e.g. Dahms, 1993; Hedin et al., 1994; Kennedy et al., 1998). Forest ecosystems are generally poor in nutrients and many studies have suggested that atmospheric deposits are significant sources of nutrients (e.g. Hedin and Likens, 1996; Okin et al., 2004; Soderberg and Compton, 2007; Pett-Ridge, 2009; Yu et al., 2015; Schuessler et al., 2018). Nutrient depletion in soils is particularly high in tropical areas, where temperature and precipitation combine to intensively leach nutrients from rocks and soil. In such contexts, the soil is usually strongly impacted by atmospheric inputs (e.g. Whipkey et al., 2000; Kurtz et al., 2001; Poszna et al., 2002; Pett-Ridge et al., 2009b). Cation nutrients, essential for plants, are thus expected to be strongly influenced by atmospheric inputs in highly weathered soils. Several studies conducted in Hawaii (Kennedy et al., 1998; Chadwick et al., 1999; Stewart et al., 2001), along chrono- and climato-sequence gradients, have shown that the more soils are leached, the more associated plants are influenced by atmospheric inputs. Other studies conducted in tropical areas of Costa-Rica (Bern et al., 2005; Porder et al., 2006) have shown that the soil-nutrient pool could still be influenced by bedrock weathering. The authors have suggested that rock-derived input was maintained by high erosion rates or deep plant roots.

The transport of African dust into the Caribbean basin is relatively well documented, either by measuring contemporary fluxes (e.g. Prospero et al., 1981; Prospero 1999) or by studying Quaternary age geological limestone records found on the western Atlantic islands of Barbados, the Florida Keys, and the Bahamas (e.g. Muhs et al., 1990; 2007). However, the number of soil record studies examining the impact of Saharan dust inputs on nutrient cycling over pedogenic timescales of hundreds to

thousands of years is limited. Studies conducted in the Luquillo Mountains in Puerto Rico (Pett-Ridge et al., 2009a; McClintock et al., 2015) have revealed that Saharan dust contributes significantly to nutrient inputs into weathered soils. Recent studies (Dessert et al., 2015; Clergue et al., 2015; Fries et al., 2019) have also tended to show that the soils of Guadeloupe can be strongly impacted by atmospheric deposits. These few studies did not take into account internal nutrient cycles in the watershed (e.g. litterfall, leaf excretion) and did not focus on the influence of dust on plants. However, the characterization of these cycles is important from the perspective of ecological theory and the understanding of Earth's Critical Zone.

As it is impossible to directly measure the cation-nutrient flux between rock, soil and vegetation, base cation cycles in forested ecosystems are not straightforward to characterize. Sr and its radiogenic isotopes have been shown to be proxies for cation-nutrient cycling in the atmosphere-soil-plant system (e.g. Capo et al., 1998; Bern et al., 2005; Belanger et al., 2012; Stille et al., 2012). As calcium has a hydrate ionic radius and an ionic charge similar to those of Sr, its behaviour can be deduced from the $^{87}Sr/^{86}Sr$ ratio. K and Mg chemistry differs from that of Ca and Sr, but these lithophile elements ultimately originate from the same sources. Their behaviour can be inferred from Sr isotope data combined with on site element flux calculations. The efficient use of Sr isotopes as a cation-nutrient cycle proxy necessitates that different Sr sources exhibit different $^{87}Sr/^{86}Sr$ ratios.

In Guadeloupe, possible common sources of Sr and base cation nutrients (volcanic rock, sea salt and Saharan dust) differ in Sr isotopic signature. The $^{87}Sr/^{86}Sr$ ratio of volcanic bedrock is between 0.70341 and 0.70382 (White and Patchett, 1984; White and Dupré, 1986). The signature of sea salt is 0.70917 (e.g. Dia et al., 1992) and the $^{87}Sr/^{86}Sr$ mean ratio of Saharan dust is 0.71788 (Biscaye et al., 1974; Grousset et al., 1988; Grousset et al., 1992; Rognon et al., 1996; Grousset et al., 1998; Pett-Ridge et al., 2009). We looked at Sr isotopes, Nd isotopes, and base cation nutrients to identify their sources. Like Sr, Nd isotope ratios are used to trace Nd sources, as they are not affected by biological and weathering processes (e.g. Liu et al., 2013). The Nd signature in volcanic rock from Guadeloupe ranges from 3.02 to 5.05 (White and Patchett, 1984; White and Dupré, 1986) and the signature of Saharan dust varies

between -10.5 and -14.5 (Grousset et al., 1992; Dia et al., 2006). Nd and Sr differ in their mobility (Nd is less mobile than Sr) and are distributed differently in surface compartments, thus the comparison between these two isotopic systems provides complementary information on constraints in the study area.

In this study we report Sr isotope ratios in all compartments of a small catchment (rainfall, throughfall, soil solution, bulk soil, unweathered rock, river water, litter and atmospheric dusts) and Nd isotope ratios of soils and unweathered rock. The catchment is located in the tropical rainforest of Guadeloupe, in the Caribbean (FWI). This area is covered by highly weathered soils built on mono-lithological volcaniclastic deposits. Despite the poverty of the soils (Buss et al., 2010; Clergue et al., 2015), a dense rainforest is developed on it (Rousteau et al., 1994, 1996). The aims of this study are to: 1) Track sources of cation nutrients (Ca, Mg, K) of the rainforest of Guadeloupe developed on a highly weathered soil; 2) Quantify the vegetation recycling of cation nutrients; 3) Identify the origin of "rock-derived" cation-nutrient pool in the soil and give constraints on regolith development.

## 2. Site description

The studied catchment (16°17'N, 61°70'W) is located on Basse-Terre Island, the volcanic part of the Guadeloupe archipelago in the French West Indies (Fig. 1). The Quiock Creek drains a watershed of 8 ha, ranging from 200 m to 350 m in altitude, located in the primary tropical rainforest of the Guadeloupe National Park. The Quiock Creek catchment is monitored by the ObsErA observatory (OZCAR research infrastructure; Gaillardet et al., 2018) dedicated to the study of weathering and erosion processes under tropical climatic conditions (Clergue et al., 2015; Lloret et al., 2016; Fries et al., 2019; Guérin et al., 2019).

The climate on site is characterized by high mean annual temperature (25°C) and precipitation (3500 $mmyr^{-1}$). The mean annual runoff is 1,130 mm. Evapotranspiration is high, between 60 and 70% (Clergue et al., 2015; Guérin et al., 2019) and tropical storms and hurricanes contribute significantly to the hydrology of the site (Zahibo et al., 2007).

Quiock Creek is covered by a very thick ferralitic soil (>15 m thick; Colmet-Daage and Bernard, 1979, IRD soil map) built on Pleistocene andesitic pyroclastic deposits (Boudon et al., 1988). The regolith profile of Quiock Creek mainly consists of secondary minerals, with kaolinite/halloysite as the main mineral (95% by weight of the bulk soil; Buss et al., 2010) and is highly depleted in mobile elements (Buss et al., 2010; Clergue et al., 2015). All these features are characteristic of a highly weathered soil. Despite the high nutrient depletion of these soils, they support a tropical rainforest (Rousteau et al., 1996; Van Laere et al., 2016). This rainforest is characterized by three dominant species: *Amanoa caribaea Kr. and Urb*. (Phyllanthaeae)*, Tapura latifolia Benth* (Dichapetalaceae) *and Dracryodes excelsa Vahl* (Burseraceae). The litter flux produced by this oldgrowth rainforest was determined each two weeks using 10 litter traps of one square meter size each monitored for two years (2011–2013). Annual litter flux reached 7.8 $t.ha^{-1}.yr^{-1}$ of dry matter (Rousteau, 2014), comparable to the rainforest flux in northeastern Puerto Rico (Weaver and Murphy, 1990). The litter production is seasonal, with the highest litter fall occurring in June-August (40% of the annual litter fall). Finally, the biomass measured on site is equal to 376.8 $t.ha^{-1}$ (Rousteau, 2014).

Atmospheric inputs to the watershed come in two forms: wet deposits and dry deposits. Wet deposits consist of rainfall, while dry deposits include sea salt aerosols, Saharan dust and volcanic ash. Because of the location of the study site in the heart of the National Park, anthropic contributions are negligible.

One of the peculiarities of the Caribbean is the major input of Saharan dust (SD) up to 100 $kg.ha^{-1}.yr^{-1}$ measured in Guadeloupe (J. Molinié, personal communication) which is consistent with amounts reported in the literature for the Caribbean basin (Glaccum and Prospero, 1980; Mahowald et al., 2006; Pett-Ridge et al., 2009; Yu et al., 2015). Throughout the Caribbean region, Saharan dust is deposited on the ground or on the canopy by rain. These dust deposits are mainly composed of mica/illite and quartz (Prospero et al., 1970; Glaccum and Prospero, 1980). For instance, in the Quiock Creek soil profile, the dull aspect of quartz, characteristic of aerial transport, suggests that Saharan dust is likely the source of quartz.

Another exogenous input to the top soil comes from the neighbouring volcano Soufriere Hills on Montserrat, located 86 km NW of Guadeloupe. It erupted on July 18, 1995, after a century of quiescence. Since 1995, six recognized ash fall episodes have impacted Guadeloupe (www.mvo.ms; activity report of OVSG 2000). The two most important events took place in September 1996 and February 2010 and produced ash-fall deposits on Guadeloupe that were thicker than 1 mm, corresponding to fluxes of about 50 to 100 g $m^{-2}$ of ash each (Cadelis et al., 2013; OVSG reports). The volcanic ashes were mainly composed of crystalline silica, mostly cristobalite (Baxter et al., 1999).

All these atmospheric sources (sea salt and dust) have been shown to highly impact soil in the Caribbean Basin (*e.g.* Borg and Banner, 1996; Herwitz et al., 1996; Muhs et al., 2009; Pett-Ridge et al., 2009; Opfergelt et al., 2012; Clergue et al., 2015; Dessert et al., 2015; Fries et al., 2019).

## 3. Sample collection

All compartments of the watershed were sampled between 2011 and 2013. Water samples consisted of rainfall, throughfall, soil solution and river water, and solid samples consisted of soil, rock, litter and dust.

### 3.1. Water samples

We collected water samples during contrasting hydrological periods. River samples (QC, n=39) were collected manually once a month and more frequently during six field trips. Rainfall (RF, n=9), and throughfall (TF, n=48) were sampled during six field trips between 2011 and 2013. They both were collected in polypropylene bottles with a funnel located one meter above the ground in order to avoid contamination from soil particles. Rainfall were collected on site on the roof of the “Maison de la Forêt” (RF-MF) or at the “Observatoire Volcanologique et Sismologique de Guadeloupe” (RF-OVSG). These samples correspond to several rainfall events cumulated over 1 to 5 days, depending on the sample. Throughfall waters were collected by three collectors randomly positioned in the Quiock Creek catchment (collector n°1 to n°3) and were sampled every 1 to 5 days, depending on the sample. Soil

177 solutions (SS) were sampled using nested tension lysimeters equipped with porous ceramic cups
178 located between 15 and 823 cm in depth (Buss et al., 2010). These soil solutions were sampled each
179 month and the sampling dates selected for isotopic measurement were 10-26-2012 and 06-28-2013.
180 Conductivity and pH were measured on site for the Quiock Creek samples and after collection at the
181 OVSG for the other samples. For alkalinity measurements, non-filtered 20 mL aliquots were used. The
182 remaining water was filtered through 0.2 µm cellulose filters and divided into two subsamples. One
183 non-acidified aliquot was stored in polypropylene bottles and used for anion and silica analyses. The
184 second aliquot was acidified (2% $HNO_3$), stored in polypropylene bottles and used for cation, trace
185 element and Sr isotope measurements. Strontium isotopic compositions were measured on 26
186 selected samples corresponding to 3 samples of rainfall, 6 samples of throughfall, 4 samples of stream
187 water and 13 samples of soil solution.

188 3.2. Solid samples

189 We analyzed andesite (04-GW-12) and basalt (00-GU-44 and 03-GU-75) samples from Samper et al.
190 (2007) to characterize the unweathered parent rock (Fig. 1). A soil profile (n=27) was collected with a
191 hand-auger down to 12.5 m depth during lysimeter installation in 2007 (Buss et al., 2010). We collected
192 Saharan dust during a dust event deposit on July 1 and 5, 2013. It corresponds to rainfall particulate
193 matter obtained by filtration on a 0.2 µm cellulose filter. The filter was then dried and stored in a Petri
194 dish. We also analysed 5 samples of litter, collected during one of the most productive periods
195 (between June 10 and 24, 2011). “Leaves 1” corresponds to a mixture of litter from different species
196 (collected in the same litter collector) whereas “Leaves 2” corresponds to *Amanoa caribaea* leaves only.
197 “Branches 1” and “Branches 2” correspond to a mixture of branches collected in two different litter
198 collectors. Finally, “Roots” (April 2012) are from *Amanoa caribaea*.

199

200 **4. Analytical methods and flux calculation**

201 4.1. Solid sample digestion

Soil and litter samples were first dried in an oven (60°C) for 3 days and crushed in an agate mortar (soil samples) or in a ball mill (litter samples). Soil and rock samples (100 mg) were dissolved in a mixture of $HNO_3$/HF for 2 days at 120 °C. This mixture was then evaporated and dissolved twice in 2mL 6N HCl and finally stored in 1N HCl. Saharan dust samples collected on cellulose filters underwent an initial step of filter digestion in diluted 5N $HNO_3$ at 100°C for 1 day and were treated with the same protocol as for rock and soil samples. Litter samples (500 mg) were first dissolved in 10 mL of 16N $HNO_3$ in 50 mL Teflon beakers for 24h at room temperature and then digested in a DigiPREP block digestion system for another 24h at 90°C. After an evaporation step at 60°C, the samples were dissolved once more in 16N $HNO_3$ for 24h at 90°C. Finally, after evaporation, 0.5 mL HF/ $H_3BO_3$ were added to fully dissolve the phytoliths. These samples were then stored in 50 mL of 2N $HNO_3$.

### 4.2. Major and trace element analyses

We measured base cations by ICP AES (Thermofisher iCap 6200 series) at the Institut de Physique du Globe de Paris (IPGP). Anions in soil solutions were measured with a Dionex DX 120 chromatograph at the IPGP and the OVSG/IPGP. We quantified Sr concentrations using HR-ICP-MS (Element II ThermoScientific) at IPGP. The limit of quantification is 20 ppt and repeated measurement of the SLRS-5 standard lead to an external reproducibility of 3%.

Major elements in solid samples were measured by ICP AES (Thermofisher iCap 6200 series) at the IPGP. Trace elements in solid samples were measured with an ICP-MS X series mass spectrometer (Thermo Electron) at the Institut des Sciences de la Terre de Paris (ISTeP) of the Université Pierre et Marie Curie. We followed the bracketing method using BEN rock standards for bracketing and BEN, GSN and LKSD2 to validate the measurements. The standard values measured in this study are compared to the certified values to validate the data (Table S1). We measured major element and Sr concentrations in litter samples using a calibration curve, such as for water samples. The accuracy of this measurement was checked by repeated analyses of a vegetation standard NIST SRM 1515.

### 4.3. Sr and Nd purification

Sr and Nd isotope analyses were performed on the Neptune multicollector ICP-MS (Thermo Scientific) at IPGP using the Apex sample inlet system. A prior step of purification is needed in order to avoid a matrix effect during measurement.

The separation of Sr from the rest of the matrix was automated for water samples with HPIC (High Performance Ion Chromatography) as fully described in Meynadier et al. (2006). Sr contained in solubilized solid samples was separated from the rest of the matrix on Sr-Spec resin in 3N $HNO_3$ media. The elution step was performed with milliQ $H_2O$. The resin was replaced after each separation to avoid memory effects. The purified solution of Sr was evaporated and dissolved in 0.05N $HNO_3$ for isotopic measurement. The minimum amount required for Sr isotopic measurement is 50-100 ng Sr in 1 mL.

For Nd separation, a two-step procedure was applied (Richard et al., 1976; Caro et al., 2006). First, rare earth elements were separated from the rest of the matrix on TRU-Spec resin in 2N $HNO_3$ media. Then, the separation of the different rare earth elements was performed on Ln-spec resin in 0.25N HCl media. The purified Nd solution was evaporated and dissolved in 3N $HNO_3$ for isotopic measurement. The minimum amount required for Nd isotopic measurement is 50 ng Nd in 1 mL.

### 4.4. Sr and Nd isotope analyses

For Sr, the method used corresponds to the measurement of 100 ratios of 4 second iteration time per sample or standard. Mass interferences with Kr (84 and 86) were corrected using $^{83}Kr/^{84}Kr$ and $^{83}Kr/^{86}Kr$, measured in the blank at the beginning of each session. Mass interference with Rb (87) was corrected using the $^{85}Rb/^{87}Rb$ ratio measured in a low concentrated Rb solution (2.5 ppb) after Kr measurement. The mass bias was corrected using the $^{86}Sr/^{88}Sr$ ratio of 0.1194. Each measurement was normalized to the NBS value certified as $^{87}Sr/^{86}Sr = 0.71025$, which was measured every 3 samples. The standard error based on repeated measurement of the NBS standard was 2% = 0.00001.

The εNd was calculated relative to the CHUR (Chondritic Uniform Reservoir) as follows:

$$\varepsilon Nd = \left(\frac{^{143}Nd/^{144}Nd_{Sample}}{^{143}Nd/^{144}Nd_{CHUR}} - 1\right) \times 10000 \quad (1)$$

The CHUR value is 0.512638 (Jacobsen and Wasserburg, 1980). The method used corresponds to the measurement of 100 ratios of 4 second iteration time per sample or standard. Mass interferences with Sm (144, 148 and 150) were corrected using $^{147}Sm/^{144}Sm = 4.83870$. The mass bias was corrected using the $^{146}Nd/^{144}Nd$ ratio of 0.72190. Each measurement was normalized to the NIST value certified as $^{143}Nd/^{144}Nd = 0.511418 \pm 6 \cdot 10^{-6}$ (Caro et al., 2006), which was measured every 3 samples. The external error was 0.18 ε (2σ).

### 4.5. Cation flux and residence time calculation

Elemental fluxes were obtained by multiplying the water/matter flux by the mean concentrations or determined from the following equations. Water fluxes were determined in Clergue et al. (2015). Throughfall water flux is 3079 mm $yr^{-1}$. The Quiock Creek discharge ranges between 150 and 400 L $min^{-1}$ with a mean value of 172 L $min^{-1}$, corresponding to a runoff of 1130 mm $yr^{-1}$. Dry matter litter flux reaches 7.8 t $ha^{-1}$ $yr^{-1}$ (Rousteau 2014).

Throughfall elementary fluxes ($F_{TF}$) are described by equation 2, where $F_{EX}$ is the flux of cations exuded by plants, and $F_{RF}$ the rainfall flux.

$$F_{TF} = F_{EX} + F_{RF} \quad (2)$$

The rainfall compartment is influenced by both sea salt aerosols ($F_{SW}$) and Saharan dust leaching ($F_{SD}$) and $F_{RF}$ is equal to:

$$F_{RF} = F_{SW} - F_{SD} \quad (3)$$

We consider that the flux of Cl in throughfall ($F\text{-}Cl_{TF}$) is exclusively from rainfall. $F_{RF}$ is determined from the $F\text{-}Cl_{TF}$ and (X/Cl) rainfall ratios:

$$F_{RF} = F\text{-}Cl_{TF} \times (X/Cl)_{RF} \quad (4)$$

with $Na/Cl_{RF} = 0.63$, $Ca/Cl_{RF} = 0.09$, $Mg/Cl_{RF} = 0.09$, $K/Cl_{RF} = 0.05$ ; $1000Sr/Cl_{RF} = 0.56$ (mean mass ratio determined from rainfall data; see following section)

and $F_{EX}$ is equal to:

$$F_{EX} = F_{TF} - F_{RF} \quad (5)$$

Assuming that all the Cl flux in throughfall has a sea salt origin, we used F-$Cl_{TF}$ and X/Cl sea salt ratios ($Na/Cl_{SW}$ = 0.86, $Ca/Cl_{SW}$ = 0.02, $Mg/Cl_{SW}$ = 0.10, $K/Cl_{SW}$ = 0.02, $1000Sr/Cl_{SW}$ = 0.16 and mass ratio from Brewer et al., 1975) to determine $F_{SW}$ for each cation:

$$F_{SW} = F\text{-}Cl_{TF} \times (X/Cl)_{SW} \quad (6)$$

and $F_{SD}$ is equal to:

$$F_{SD} = F_{RF} - F_{SW} \quad (7)$$

The vegetation flux ($F_{VEG}$) is described by equation 8, where $F_{EX}$ is the flux of cations exuded by plants, and $F_{LF}$ the litter fall flux.

$$F_{VEG} = F_{EX} + F_{LF} \quad (8)$$

The standing stock of cations in the forest (Stock) is determined from biomass (376.8 $t.ha^{-1}$; Rousteau et al., 2014) and mean cationic concentrations into plants. The residence time ($T_{res}$) of each element in the vegetation is determined by the following equation:

$$T_{res} = Stock / F_{VEG} \quad (9)$$

## 5. Results

All the compartments of the catchment were characterized for their element concentrations and isotopic compositions. Table 1 presents results of major elements and Sr concentrations only in water samples for which Sr isotopic composition was measured. A full list of the concentrations of major cations we have used in this paper are taken from Clergue et al. (2015) of which the range in

concentrations, means and median values are summarized in Table 2. New trace element and isotopic compositions for solid samples are presented in Table 3.

### 5.1. Atmospheric samples

The pH of rainfall ranged from 4.1 to 5.7 (Clergue et al., 2015). The major cation in rainfall was Na, whose concentration varied between 41 and 165 µmol/L. The mean concentration of K, Ca and Mg were 4, 7 and 12 µmol/L, respectively. Sr concentration ranged from 9 and 39 nmol/L (Table 2S) and Sr isotopic composition varied between 0.70841 and 0.71029 (Fig. 2). These data were in agreement with previously published data in the Puerto Rican and Guadeloupean rainforests (Gioda et al., 2013; Dessert et al., 2015).

The concentrations of major elements in Saharan dust collected in Guadeloupe, were higher than those in the soil samples (except for Al and Fe; see Clergue et al., 2015) and lower than in the rock samples (Table 3). The average values for Ca (1830 ppm), Na (940 ppm) and K (5300 ppm) were lower than those reported in the literature for dust samples collected in West Africa (> 2600 ppm for Ca and Na, > 9800 ppm for K; Moreno et al., 2006). Mg concentrations around 5200 ppm were in the range of those reported in the literature (> 4600 ppm; Moreno et al., 2006). The concentration of Sr concentration was around 50 ppm, 1.5 to 5 times lower than the values reported in the literature for dust samples (Moreno et al., 2006) and 10 times higher than soil Sr concentrations. Concerning Sr isotopic data, the dust samples were the most radiogenic of all samples collected on the site. The isotopic signature, around 0.7187, is consistent with previous estimations and measurements (Biscaye et al., 1974; Grousset et al., 1988; Grousset et al., 1992; Rognon et al., 1996) which gave a value of 0.7179 for Saharan dust in the Caribbean (Pett-Ridge et al., 2009b).

### 5.2. Throughfall samples

The pH of the throughfall was slightly higher than that of the rainfall, ranging from 5.1 to 6.3 (Clergue et al., 2015). The major cation in the throughfall was Na, whose concentration varied between 17 and 264 µmol/L (Table 2). Mean concentration of K, Ca and Mg were 39, 17 and 17 µmol/L respectively. Sr

concentration ranged from 8 and 136 nmol/L (Table S2) and Sr isotopic composition varied between 0.70953 and 0.70978 (Table 1, Fig. 2). These data were in agreement with the ranges published in the literature for tropical rainforests (e.g. Forti and Neal, 1992; McDowell, 1998).

The K/Cl ratio in throughfall was ten times higher than the K/Cl ratio in rainfall, attesting to a strong enrichment of K in throughfall (Fig. 3). To a lesser extent, Sr, Ca and Mg were also enriched in throughfall. The enrichment of throughfall compared to rainfall indicates that these elements are partially released by plants. This exudation process has been largely described in the literature (Vitousek and Sanford, 1986; Dezzeo and Chacon, 2006).

Throughfall is slightly more radiogenic than sea salt (Fig. 2). This observation can be explained by a mixture in throughfall of sea salt Sr and Sr from Saharan dust leachates or plant exudates. It is impossible to distinguish between the two latter sources only on the basis of Sr isotopes.

### 5.3. Litter samples

Major element concentrations in litter samples were very different from concentrations in the other solid samples (Table 3). The most abundant element in the litter was Ca, with concentrations ranging between 1 and 3%. This is more than 100 times the Ca concentration in the soil and is similar to the parent rock Ca concentration. The K concentration, intermediate between 0.1 and 1.1%, and the Mg concentration, ranging between 0.2 and 0.6%, were also higher than the K and Mg concentrations in the soil. These concentrations are consistent with values in the literature for litter samples (e.g. Liao et al., 2006; Riotte et al., 2014). Similarly, the Sr concentration in the litter varied from 80 to 200 ppm, which is one or two orders of magnitude higher than the Sr concentration in the soil (up to 13 ppm). The isotopic signature of the litter varied between 0.70966 and 0.71019 (Fig. 2). This signature differed from the $^{87}Sr/^{86}Sr$ ratio of local bedrock, but was similar to that of samples of vegetation growing on highly depleted volcanic soil as reported in the literature (Whipkey et al., 2000; Stewart et al., 2001; Chadwick et al., 2009).

### 5.4. Soil solution samples

345 The soil solutions were acidic, with pH values ranging from 4.2 to 5.4. This can be explained by the low
346 cation content, which plays a key role in neutralizing the acidity of soil solutions. Na and Cl were the
347 most abundant elements, with mean concentrations of 179 µmol/L and 199 µmol/L, respectively (Table
348 2). Average Mg, K and Ca concentrations were 24, 5 and 3 respectively. Sr concentrations in soil
349 solutions ranged between 7 and 101 nmol/L (Table S2), and isotopic composition varied between
350 0.70996 and 0.71097 (Table 1). Soil solutions were more radiogenic than local rocks and sea salts,
351 attesting to an exogenous source of Sr in the soil solution (Fig. 2). In superficial soil horizons (up to 90
352 cm), Sr concentrations were systematically higher than in the deeper horizons (mean value of 53 and
353 16 nmol/L respectively). To a lesser extent, Ca and Mg were also slightly higher in superficial horizons
354 than in the deepest. On the contrary, K concentrations were constant over the entire soil profile.

355 Fig. 3 shows the cation concentrations normalized to Cl for all dissolved samples. Na/Cl ratios were
356 relatively homogeneous in all water samples and close to the sea salt ratio. In general, soil solutions
357 were depleted in nutrient cations compared to throughfall. This was particularly true for K, which was
358 probably due to efficient K uptake by plant root systems and microorganisms in the first few
359 centimeters of soil. As previously noted, soil solutions of superficial horizons were slightly enriched in
360 Sr, Ca and Mg compared to deeper soil solutions, which indicates a potential atmospheric source of
361 cations. It was even observed that the surface solutions were sometimes enriched in Mg with respect
362 to throughfall.

363 5.5. Soil and rock samples

364 The soil profile is characterized by a very high proportion of secondary minerals (95% wt. of secondary
365 minerals and 70 %wt. of kaolinite and halloysite; Buss et al., 2010). The chemical composition of the
366 soil indicated that it was highly depleted in mobile cations compared to unweathered rock in
367 Guadeloupe (Table 3). For example, the Ca concentration varied from 23 to 306 ppm, which
368 corresponds to about 100% depletion compared to volcanic rock, which contains 4.85% to 7.45% of Ca.
369 Sr concentration in soil varied between 2 and 13 ppm and was very low compared to unweathered rock

(Table 3). To correct for dilution effects and volume change, Sr concentration in the soil samples was normalized to an immobile element (Ti). Fig. 4 presents mass transfer coefficient (τ) values for Sr:

$$\tau Sr = [(Sr/Ti)_{soil} / (Sr/Ti)_{rock}] -1 \quad (10)$$

τSr was negative, representing the depletion of Sr in soil compared to unweathered rock. Sr had a depletion rate of around 98 ± 2%. The soil profile was systematically less depleted in its first 15 cm and at depths of 305 cm, 427 cm, 1219 cm and 1250 cm. These depths corresponded to horizons enriched in quartz and K-feldspar.

The entire profile was more radiogenic (0.70677 – 0.71527) than the unweathered volcanic rock sampled in Guadeloupe (Fig. 2 and 4). Quartz horizons exhibited the highest Sr isotopic ratio. This observation attests of exogenic source(s) of Sr to the soil. The εNd of the profile varied between -8.39 and 2.44 and was different from unweathered rock ranging from 4.34 to 5.45 (Table 3). The Nd signature of the quartz horizons was very negative and attested again of an exogenic contribution of Nd to the profile.

### 5.6. Quiock Creek water samples

Conductivity in Quiock Creek ranged from 22.5 to 68.2 µS and pH was acidic, ranging from 4.3 to 5.9 (see Clergue et al., 2015). The major cation was Na, with a mean concentration of 234 µmol/L. Mean concentrations of K, Ca and Mg were 5, 10 and 29 µmol/L, respectively (Table 2). Sr concentration ranged from 35 and 70 nmol/L (Table S2) and Sr isotopic composition varied between 0.70922 and 0.70939.

## 6. Discussion

### 6.1. Vegetation cycling

#### 6.1.1. Impact of atmospheric deposits on the cation-nutrient budget

A key question is to what extent atmospheric deposition (wet and dry) impacts the forest's nutrient source. Many biogeochemical studies have shown that Sr, and particularly the $^{87}Sr/^{86}Sr$ isotopic ratio, is a good tracer of ecosystem Ca sources (e.g. Capo et al., 1998; Bern et al., 2005; Belanger et al., 2012; Stille et al., 2012; Pett-Ridge et al., 2009a). K and Mg chemistry differs from Ca and Sr, but these lithophilic elements ultimately originate from the same sources. It is therefore possible to acquire some qualitative information on the cycles of these elements using Sr as a proxy.

The internal water cycle of our basin is relatively homogeneous from a Sr isotopic point of view, with a mean $^{87}Sr/^{86}Sr$ ratio of 0.7097 for throughfall and 0.7104 for soil solutions (up to 12 meters deep; Fig. 2). This shows that the dissolved pool of Sr is dominated by sea salts ($^{87}Sr/^{86}Sr$ value equal to 0.7092), with a small influence of more radiogenic sources coming from Saharan dust leaching (Fig. 2). Note also that the Sr isotopic composition of litter of 0.7099 is in the range of that of the dissolved pool of Sr. This has already been well described in several studies, which have shown that vegetation exhibits the signature of the exchangeable Sr pool (e.g. Kennedy et al., 1998; Poszwa et al., 2002). Our results emphasize that atmospheric inputs contribute significantly to actively cycled Sr in the Quiock Creek basin. This hypothesis is consistent with the literature for similar contexts with highly depleted volcanic soils and strong atmospheric input (e.g. Whiptkey et al., 2000; Stewart et al., 2001; Chadwick et al., 2009; Schuessler et al., 2018). As an example, Pett-Ridge et al. (2009a) reported that the proportions of foliar Sr derived from sea salt and dust vary between 33% and 59% in the Puerto Rican rainforest. Similarly, in the Quiock Creek catchment, the $^{87}Sr/^{86}Sr$ of litter is slightly more radiogenic than sea salt aerosols, emphasizing the influence of Saharan Sr on the ecosystem.

Based on the Sr isotopic composition, the weathering of local volcanic rock seems not to contribute in the plant Sr pool. It can be deduced that this is also true for the Ca, K and Mg pools. This observation is consistent with the idea that tropical forests developed on highly nutrient-depleted soils derive their nutrients from superficial atmospheric sources and from litter recycling (Jordan, 1982). It may be for this reason that surface soil solutions are slightly less depleted in cations than deeper solutions (>91 cm; Fig. 3), reflecting the cationic inputs of throughfall, dust leaching/weathering and litter

remineralization. We also suggest that a little near-surface nutrient pool sustains the forest community of Quiock Creek.

Tropical forests are largely described as dependent on atmospheric sources, as observed in this study, but they are also known to recycle nutrients very efficiently. In the following section, we calculate the vegetation fluxes in the catchment and estimate the cation-nutrient recycling fluxes.

6.1.2. Vegetation cycling at the soil-plant profile scale

Nutrients contained in plants are released during leaf excretion, litter leaching and litter decomposition. These bio-available elements are partly taken up by the vegetation from the soil solution and, therefore, are recycled. The proportion of nutrients recycled by plants depends on the amounts of available nutrients in the soil. As an example, the study by Holmden and Belanger (2010) shows that in a Boreal forest ecosystem, the proportion of recycled Ca from litter fall can represent from 80% and 90% of the annualized Ca inputs to the forest Ca cycle. The authors also note that the proportion of recycled Ca increases with decreasing weathering flux.

The internal-cationic fluxes calculated in the Quiock Creek catchment are summarized in Table 4 and Fig. 5. The vegetation flux ($F_{VEG}$) varies between 8.4 $kg.ha^{-1}.yr^{-1}$ for Na and 141.5 $kg.ha^{-1}.yr^{-1}$ for Ca and represents the biggest elemental flux, except for Na. These results are in agreement with those of the review by Proctor et al. (1987) on primary rainforests and the study by McDowell (1998) in a Puerto Rican rainforest. For Ca, Mg and Sr, most of the vegetation flux is provided by litter fall. Concerning K, its flux provided by leaf excretion (41.2 $kg.ha^{-1}.yr^{-1}$) is twice as abundant as the litter fall flux (20.9 $kg.ha^{-1}.yr^{-1}$). This confirms that canopy leaching is the main source of K for the top soil (e.g. McDowell 1998; Riotte et al., 2014). Finally, the Na flux released by vegetation is relatively weak compared to rainfall flux. Na is not a nutrient for plants and it exhibits conservative behaviour when rainwater passes through the canopy. We note that for Sr, K, Ca, and, to a lesser extent Mg, plant recycling is highly efficient. The vegetation flux ($F_{VEG}$) of Sr, K, and Ca are respectively, 20, 28 and 31 times greater than flux exported at the outlet of the basin ($F_{QC}$). The vegetation flux of Mg is 3 times greater than the flux

444 exported by the Quiock Creek. This vegetation turnover efficiency is related to the degree of soil
445 leaching and thus the nutrient pool derived from weathering minerals. In the tropical context of our
446 study, it is not surprising to observe such a high turnover, because of the nutrient paucity in soils. The
447 same range of solute turnover has been measured in the tropical watershed of Mule Hole in India
448 (Riotte et al., 2014), where vegetation recycling fluxes represented 10-15 times the exported fluxes.
449 More recently, in a tropical watershed in Sri Lanka, Schuessler et al. (2018) estimated this recycling
450 factor between 2 and 7 for Mg, 3 and 10 for Ca and 9 and 29 for K.

451 Rousteau et al. (2014) have shown that vegetation in the Quiock Creek catchment is at equilibrium with
452 respect to carbon. If the ecosystem is close to equilibrium, the nutrient fluxes taken up would be equal
453 to $F_{VEG}$ (litter fall + leaf excretion). Numerous studies (e.g. Proctor, 1987) have shown that in tropical
454 rainforests, decomposition is invariably rapid and that litter turnover takes less than a year. Even though
455 we did not measure the decomposition rate of litter, our field observations confirm the speed of this
456 process. From the standing stocks of cations in the forest and the annual-cationic $F_{VEG}$ fluxes (Table
457 4), we determined the residence time ($T_{res}$) of each element in the vegetation. The element presenting
458 the shortest residence time in the vegetation is K, namely 16 years. This residence time is consistent
459 with the 10 year period determined for K in Puerto Rican forest (McDowell 1998). This short residence
460 time is justified by the fact that K is one of the most important elements for plant metabolism (as a
461 catalytic agent for carbohydrate synthesis and the transfer of other nutrients) and is abundantly
462 excreted by the leaves. For other elements, the residence time is slightly longer than those determined
463 for K: 44.6 years for Sr, 44.9 for Ca, 45.7 for Mg and 48.2 for Na. These results highlight that vegetation
464 recycling dominates the nutrient cycle, and, in light of the Sr isotopic signature, we can deduce that
465 these nutrients have the particularity of being initially of atmospheric origin. Therefore, the Quiock
466 Creek ecosystem is sustained by a little near-surface nutrient pool, which seems disconnected from the
467 deep bedrock.

468 Our study is a first step in the characterization of biogeochemical cycles at the plant-soil scale in the
469 Guadeloupean rainforest. To better characterize and quantify the nutrient recycling, it would be useful

for example, to study the seasonality of vegetation fluxes, investigate the N and P cycles, or use the isotopic fractionations of the elements involved in these biogeochemical processes (Ca, Mg, Si, B,...).

## 6.2. Soil cation-nutrient pool and weathering

### 6.2.1. Origin of cation-nutrient pool in the soil

After studying geochemical cycles at the plant-soil scale, it is necessary to study the soil profile to determine whether soil is still able to provide nutrients to the forest.

In the entire soil profile (Fig. 2), the Sr isotopic signature of the solid phase is high relative to rock, which is consistent with exogenous contributions of Sr. Fig. 6 presents the Sr isotopic signature of soil as a function of the Sr depletion rate ($\tau Sr$). The more the sample is rich in Sr, the more the soil Sr signature is radiogenic. This implies that the main source enriching the soil in Sr is more radiogenic than bedrock. The two potential sources of Sr that could enrich the soil in radiogenic Sr are: 1) Sea salts with a signature of 0.70917 (Dia et al., 1992) or 2) Saharan dust with a signature of 0.7187 (this study). This indicates that the soils are so leached that they have almost lost their original rock signature and have inherited an exogenous atmospheric signature. As previously discussed (Section 5.5) at depths of 15, 30, 305, 427, 1219 and 1250 cm, the high $^{87}Sr/^{86}Sr$ ratios (> 0.712) are correlated with the highest primary mineral content (Quartz + Feldspar), which could correspond to different dust deposit horizons. All the other soil samples are not enriched in primary minerals but, nevertheless, are characterized by Sr isotopic ratios that indicate a mixture of bedrock and exogenous atmospheric sources. This indicates that Sr derived from atmospheric deposits is transferred to the soil exchangeable pool and may be incorporated into secondary minerals. This recycled Sr in the soil exchangeable pool could be taken up by plants and reinforces the hypothesis that the nutrients involved in the Quiock Creek ecosystem are of atmospheric origin. This strong atmospheric influence on the soil profile has been described in the study by Clergue et al. (2015), devoted to Li dynamic in the same catchment. The $\delta^7Li$ measured in the soil profile also indicated that atmospheric deposition (wet and dry) was a main source of Li in the bulk soil.

Because both wet and dry atmospheric deposits are sources of radiogenic Sr, it is not possible to discriminate between sea salt and Saharan sources in soil only on the basis of the $^{87}Sr/^{86}Sr$ ratio. Coupled with Sr isotopes, Nd isotopes are useful for identifying the different contributions to the soil profile. For example, εNd of rock ranges from 4.34 to 5.45 (Table 3) and εNd of Saharan dust ranges from -10.5 to -14.5 (Grousset et al., 1992; Dia et al., 2006; Scheuvens et al., 2013; McClintok et al., 2015). Sea salt exhibits an extremely low Nd concentration and Saharan dust input seems to be the only atmospheric contribution able to shift the isotopic composition of the soil. The Nd isotopic composition of soil varies between -8.39 and 2.71 and could be explained by a mixture of rock and dust endmembers. The quartz-feldspar horizons are characterized by very negative εNd, indicating a strong Saharan Nd contribution. The amount of quartz and Nd isotopes provide two independent proxies of long-term dust additions to the soil profile. The superficial horizon (the first 30 centimetres) is a contemporary depositional surface while the other horizons attest to past deposition. The deepest quartz horizons (305, 427, 792 and 1219-1250 cm) may represent paleo-surfaces of dust deposits, interspersed between multiple events of volcanic deposition. The variable thickness of these horizons may be partly explained by a physical soil mixing process resulting from bioturbation.

In Fig. 7, the soil samples are plotted in a two-component mixing diagram for $^{87}Sr/^{86}Sr$ versus εNd. The curvature of the different mixing lines depends on the Sr/Nd ratio of each endmember. The dotted curve represents the mixing line between the unweathered rock endmember ($^{87}Sr/^{86}Sr$ = 0.7038, εNd = 4.8, Sr/Nd = 17.9; from this study and the andesite Nd content of 16 ppm from Taylor and McLennan 1985) and the Saharan endmember ($^{87}Sr/^{86}Sr$ = 0.7187, εNd = -11.5, Sr/Nd = 3.4; from this study and Grousset et al., 1998). This mixing line cannot explain the isotopic composition of the soil samples, indicating that dust is not mixed with fresh rock but with a Sr-depleted weathered rock. Four mixing lines with depleted rock endmembers are shown on Fig. 7. Their Sr/Nd ratios decreased from 10 to 0.1 in the most depleted case.

If we first consider soil horizons enriched in quartz-feldspar, this mixing model confirms that these particular layers are strongly influenced by the dust endmember. It also emphasized that the

proportion of Saharan Sr in the soil decreases with depth, from 65% in the first 15 cm, to 20% in the deepest quartz-feldspar horizons. Finally, our results show that the degree of rock depletion also increases with depth. Indeed, surface horizons (15 and 30 cm) can be explained by mixing of dust with moderately depleted rock (10<Sr/Nd<5) whereas the deeper horizons involve a mixture with a very depleted rock (Sr/Nd<1). The superficial volcanic rock signature is inherited from the deposit of volcanic ashes in Guadeloupe linked to very recent activity of neighbour volcano Soufriere Hills on Montserrat (Baxter et al., 1999; Cadelis et al., 2013). The accumulation of Saharan dust in the upper soil is also observed in quartz-diorite and volcaniclastic soils in Puerto Rico (McClintock et al., 2015), which is too far from the volcanic arc of the Lesser Antilles to be impacted by recent ash deposits. In Puerto Rico, the calculated soil dust content ranges between 0 and 8%, and Nd from dust in the upper 20 cm of soil ranges between 0 and 92% (McClintock et al., 2015), which is consistent with what we have observed in Guadeloupe.

If we now consider soil horizons non-enriched in quartz-feldspar, we note that their isotopic composition still reflects a slight influence of the dust endmember and that they have $^{87}Sr/^{86}Sr$ ratios close to those of rainfall or that are slightly more radiogenic. The rock Sr isotope signature in these horizons has been completely overprinted by the atmospheric signature (rainfall and dust-derived Sr). The slight influence of dust on the Nd signature in the entire soil profile is clear evidence for the mobilization of dust-derived Nd and its redistribution in the soil. This is especially the case for the horizons at depths of 61 and 91 cm, which do not contain quartz and felspar, but whose Sr and Nd isotope signatures are strongly influenced by the dust endmember (25 to 35%). It is possible that the Sr and Nd come from the leaching of Saharan minerals contained in the upper soil and that are reincorporated into the deeper soil levels. Even if Nd mobility is much lower than Sr mobility, it seems to increase under extreme leaching conditions. This mobilization of dust-derived Nd into highly weathered soil profiles has been observed in Puerto Rico, where the Nd isotope signature of Saharan dust has been observed noted at depths of 2 and 3 m (Pett-Ridge et al., 2009b). Our mixing model cannot explain all the data because of the influence of a third end-member, namely sea salt Sr derived

from rainwater. Because sea salts are not a significant source of Nd, the addition of sea salts does not influence the Nd isotopic composition of soil. Except for the dust horizons, andesitic and dust-derived Sr have been leached extensively and the sea salt Sr signature dominates in the entire profile.

In the Quiock Creek catchment, we observe a strong impact of atmospheric sources on the evolution of the chemical composition of the soil with depth and with time. Elements are continuously provided at the surface by fresh dust minerals on a highly depleted soil. Then, we observe a "reversed" weathering profile, with the horizon the most enriched in primary minerals (Saharan and volcanic) and having the strongest andesitic isotopic signature at the top of the soil profile. The impact of atmospheric sources on volcanic soil has been demonstrated in different tropical contexts. In a soil chronosequence in Hawaii, it was shown that the older the soils, the bigger the impact of atmospheric inputs (Kennedy et al., 1998; Whiptkey et al., 2000; Kurtz et al., 2001; Chadwick et al., 2009). Saharan dust was shown to affect soil composition in Puerto Rico (Pett-Ridge et al., 2009b; McClintock et al., 2015) and in Mount Cameroon (Dia et al., 2006). In Guadeloupe, Mg and Li isotopes reflect the influence of sea salt and dust on soil (Opfergelt et al., 2012; Clergue et al., 2015; Fries et al., 2019). Our study supports these prior observations and the need to fully account for these inputs when studying weathering and cation-nutrient cycling under tropical climatic conditions.

6.2.2. Does chemical weathering provide elements to the catchment flux?

The comparison between rainfall fluxes and output flux from Quiock Creek provides information on processes taking place in the soil. Elementary budgets (output flux – input flux) are negative (Fig. 5). This may mean that the catchment stores cation nutrients in the soil or in the vegetation. However, it can also mean that for these elements, inputs from rainfall are underestimated. In fact, their mean concentrations in rain are highly variable and hard to estimate. In any case, it means that these elements are not enriched as they move through the soil and thus there is no weathering flux for these elements in the catchment. The Sr isotopic composition of Quiock Creek, which is close to the sea salt aerosol signature, supports the idea that the Sr comes from atmospheric input only (Fig. 5). The fact

572 that the Quiock Creek $^{87}Sr/^{86}Sr$ ratio is very different from the volcanic rock signature, indicates that
573 the local rock no longer contributes to the weathering flux. The absence of weathering flux in the
574 Quiock Creek catchment and its peculiar Sr isotopic composition are linked with the intense weathering
575 of the soil, which is highly depleted in major elements (Clergue et al., 2015). This situation is peculiar
576 in Guadeloupe, as in all other catchments studied, the weathering flux is equivalent, or even twice as
577 high, as the rainfall flux (Dessert et al., 2015). This situation is also peculiar in the Caribbean, for
578 example in Puerto-Rico, where numerous catchments are surveyed by the USGS. In the Puerto-Rican
579 catchments, which are subject to the same climate and are covered by rainforest, soils are not as
580 depleted as in Guadeloupe (e.g. Ferrier et al., 2010). The Rio Icacos basin in Puerto Rico is the site of
581 the highest measured chemical solute fluxes for a catchment on granodiorite (Turner et al., 2003).

582 Clergue et al. (2015) showed that in this catchment, part of the weathering flux of Li originates from
583 the main secondary mineral dissolution (i.e. kaolinite). Using the kaolinite dissolution rate (Carroll et
584 al., 1988), the authors showed that kaolinite dissolution can explain the weathering flux of Li measured
585 on site. The same calculations were made for Mg and Sr, using the average concentration of those
586 elements in kaolinite. They show that kaolinite can provide Mg and Sr by dissolution, with a respective
587 flux of 0.012 $kg_{Mg}$ $ha^{-1}$ $yr^{-1}$ and 0.002 $kg_{Sr}$ $ha^{-1}$ $yr^{-1}$. However, these fluxes are much lower than the
588 rainfall fluxes and consistent with the absence of measurable weathering flux for some major elements
589 and Sr.

## 7. Conclusion

In the Quiock Creek catchment, a large range of $^{87}Sr/^{86}Sr$ and εNd values is observed despite the small scale of observation. Sr isotopic composition varies from 0.70677 in deep bulk soil samples to 0.71882 in dust samples. The Nd isotopic composition varies just as much, between -8.39 in near-surface soil samples to 2.71 in deeper soil (732 cm depth). For the Saharan dust endmember, we used a mean εNd value of -11.5, determined from the literature. These large isotopic ranges, coupled with major and trace elements, have helped to better understand nutrient dynamic in tropical ecosystems in Guadeloupe.

The regolith profile was built on pyroclastic deposits, but, because of extreme leaching, it has almost lost its original andesitic signature and inherited an exogenous atmospheric signature. Only Saharan dust is likely to have influenced the Nd balance throughout the entire 12m-thick profile, while the Sr balance is influenced by both Saharan dust and sea salt aerosols. Sr and Nd isotopes, combined with mineralogy and mobile element concentrations in the regolith, argue for a multi-layered soil profile which has been built by successive volcaniclastic episodes, separated by periods of dust deposition. Deep horizons enriched in quartz-felspar are then interpreted as paleo-soils impacted by Quaternary Saharan dust deposits, whereas the near-surface soil horizon is currently impacted by fresh dust deposits. Our results show that only the chemical weathering of the near-surface fresh minerals can provide nutrients to the ecosystem, the deeper regolith (> 30 cm) being nutrient depleted. However, this dust weathering flux is too low to sustain the tropical forest ecosystem.

The cationic mass balance at the catchment scale and the Sr isotopic signature of Quiock Creek indicate that cation and Sr fluxes are of atmospheric origin. Thus, in this highly weathered catchment, the original andesitic bedrock no longer participates in the weathering fluxes of Quiock Creek. This conclusion leads us to question the notion of “bedrock” in catchment involving on a deep weathered formation. Is it still an andesitic bedrock or is it now a lateritic bedrock?

The dissolved Sr cycle at the catchment scale is mainly dominated by sea salts, with a small contribution of Sr coming from the Saharan dust leaching. The vegetation exhibits the signature of the dissolved pool of Sr, indicating that the nutrient pool derives from atmospheric inputs.

At the soil-plant scale, the cation-nutrient fluxes provided by vegetation (litter fall + leaf excretion) are major compared to input and output fluxes. The Ca, K, Sr and Mg fluxes each year in the vegetation are, respectively, 31, 28, 20 and 3 times greater than the exported fluxes at the outlet of the basin. The residence time of nutrients in vegetation is 16 years for K and close to 45 years for Sr, Ca and Mg. These results emphasize the highly efficient plant turnover that dominates the nutrient cycle in the Quiock Creek catchment.

This first characterization of biogeochemical cycles in a Guadeloupean forest suggests that the forest community of Quiock Creek is sustained by a small near-surface nutrient pool, disconnected from the deep andesitic bedrock.

**Acknowledgements**

This work has been financially supported by the INSU-CNRS and the Région Guadeloupe. Parts of this work were supported by the IPGP multidisciplinary program PARI and by the Paris–IdF region SESAME Grant no. 12015908. This work could not have been done without logistical support from 1) both INSU-CNRS observatories in Guadeloupe run by the IPGP: the Observatoire de l'Eau et de l'Erosion aux Antilles (OBSERA) and the Observatoire Volcanologique et Sismologique de Guadeloupe (OVSG) and, 2) the Parc National de Guadeloupe (PNG). We thank in particular N. Liagre, M. Valy and F. Bastaraud from PNG for their assistance with the field work. We also thank X. Quidelleur and P. Lahitte (Paris Sud 11 University) for providing us with rock samples from Guadeloupe. Major element concentrations from water and solid samples were measured by L. Cordier and C. Gorge. Thanks are extended to B. Caron from IsTeP-UPMC and J.-L. Birck, A. Cogez, L. Faure, A. Michel, M. Tharaud from IPGP for their analytical assistance. The equipment and services of the Laboratoire de biologie et de physiologie

végétale de l'Université des Antilles was used for the biological and ecological aspects of the study. We thank M. Daullet for his assistance in the laboratory. Special thanks to V. Virapin, who processed and weighed most of the collected litter samples and E. Mira who made and placed the litter traps. This study greatly benefited from comments from A. Cogez, M. Dulormne, F. Bussière, J. Molinié and R. Losno. We gratefully acknowledge Susan Johnson for her helpful comments on the original version of this paper. We have a special thought for our colleague and friend Agnès Michel, who passed away in 2018. She was involved in the solid sample analyses and was always keen to develop new analytical experiments. We gratefully acknowledge two anonymous reviewers and the editor for their helpful and critical comments on the original manuscript. IPGP contribution # 4079.

## References


Baxter, P.J., Bonadonna, C., Dupree, R., Hards, V.L., Kohn, S.C., Murphy, M.D., Nichols, A., Nicholson, R. A., Norton, G., Searl, A., Sparks, R.S.J., Vickers, B.P., 1999. Cristobalite in volcanic ash of Soufriere Hills Volcano, Monserrat. British West Indies. Science 283, 1142-5.

Bélanger, N., Holmden, C., Courchesne, F., Côté, B., Hendershot, W.H., 2012. Constraining soil mineral weathering 87Sr/86Sr for calcium apportionment studies of deciduous forest growing on soils developed from granitoid igneous rocks. Geoderma 185-186, 84-96.

Bern, C.R., Townsend, A.R., Lang Farmer, G., 2005. Unexpected dominance of Parent-materiel strontium in a tropical forest on highly weathered soils. Ecology 86, 626-632.

Biscaye, P. E., Chesselet, R., Prospero, J. M., 1974. Rb-Sr, 87Sr/86Sr isotope system as an index of provenance of continental dusts in the open Atlantic Ocean. Journal de Recherches Atmospheriques 8, 819-829.

Borg, L.E., Banner, J.L., 1996. Neodymium and strontium isotopic constraints on soil sources in Barbados, West Indies. Geochim. Cosmochim. Acta 60 (21), 4193–4206.

Boudon, G., Dagain, J., Semet, M. P., Westercamp, D., 1988. Le massif volcanique de la Soufrière (département de la Guadeloupe, Petites Antilles). In: BRGM (Ed.), Carte géologique au 1/20.000ème.

Brewer, P. G., Riley, J. P., Skirrow, C. (1975) Chemical oceanography. Academic Press, New York,1, 417.

Buss H.L., White A.F., Dessert C., Gaillardet J., Blum A.E., Sak P.B., 2010. Depth profiles in a tropical volcanic critical zone observatory: Basse-Terre, Guadeloupe. In: Torres-Alvarado, I.S., Birkkle, P. (Eds.), Proceedings of the 13th International conference on water-Rock Interaction. Taylor & FrancisGroup, London, UK.

669 Cadelis, G., Tourres, R., Molinie, J., Petit, R.H., 2013. Exacerbations of asthma in Guadeloupe (French
670 West Indies) and volcanic eruption in Montserrat (70 km from Guadeloupe). Revue des Maladies
671 Respiratoires 30, 203-214.

672 Capo, R.C., Stewart, B.W., Chadwick, O.A., 1998. Strontium isotopes as tracers of ecosystem processes:
673 theory and methods. Geoderma 82, 197-225.

674 Caro, G., Bourdon, B., Birck, J.L., Moorbath, S., 2006. High-precision $^{142}Nd/^{144}Nd$ measurements in
675 terrestrial rocks: constraints on the early differentiation of the Earth's mantle. Geochim. Cosmochim.
676 Acta 70 (1), 164–191.

677 Carroll-Webb, S. A., & Walther, J. V. (1988) A surface complex reaction model for the pH-dependence
678 of corundum and kaolinite dissolution rates. Geochi. Cosmochim. Acta 52 (11), 2609-2623.

679 Chadwick, O. A., Derry, L. A., Vitousek, P. M., Huebert, B. J., Hedin, L. O., 1999. Changing sources of
680 nutrients during four million years of ecosystem development. Nature 397(6719), 491-497.

681 Chadwick, O. A., Derry, L. A., Bern, C. R., Vitousek, P. M., 2009. Changing sources of strontium to soils
682 and ecosystems across the Hawaiian Islands. Chem. Geol. 267(1), 64-76.

683 Clergue, C., Dellinger, M., Buss, H. L., Gaillardet, J., Benedetti, M.F., Dessert, C., 2015. Influence of
684 atmospheric deposits and secondary minerals on Li isotopes budget in a highly weathered catchment,
685 Guadeloupe (Lesser Antilles). Chem. Geol. 414, 28-41.

686 Colmet-Daage, F., Bernard, Z., 1979. Contribution à l'Atlas des départements d'Outre-mer: Guadeloupe.
687 Carte des sols de la Guadeloupe, Grande-Terre, Marie-Galante. Carte des pentes et du modelé de la
688 Guadeloupe, Grande-Terre, Marie-Galante. ORSTOM, Antilles.

689 Cuevas, E., Lugo, A.E., 1998. Dynamics of organic matter and nutrient return from litterfall in stands of
690 ten tropical tree plantation species. Forest Ecology and Management 112, 263-279.

691 Dahms, D.E., 1993. Mineralogical evidence for eolian contribution to soils of late quaternary moraines,
692 Wind River Mountains, Wyoming, USA. Geoderma, 59, 175-196.

693 Dessert, C**.,** Lajeunesse, E., Lloret, E., Clergue, C., Crispi, O., Gorge, C., Quidelleur, X., 2015. Controls on
694 chemical weathering on a mountainous volcanic tropical island: Guadeloupe (French West Indies).
695 Geochim. Cosmochim. Acta 171, 216-237.

696 Dezzeo, N., Chacon, N., 2006. Nutrient fluxes in incident rainfall, throughfall, and stemflow in adjacent
697 primary and secondary forests of the Gran Sabana, southern Venezuela. Forest ecology and
698 management 234, 218-226.

699 Dia, A., Chauvel, C., Bulourde, M., Gérard, M., 2006. Eolian contribution to soils on Mount Cameroon:
700 Isotopic and trace element records. Chem. Geol. 226, 232-252.

701 Dia, A. N., Cohen, A. S., O'Nions, R. K., Shackleton, N. J., 1992. Seawater Sr isotope variation over the
702 past 300 kyr and influence of global climate cycles. Nature 356, 786 – 788.

703 Ferrier, K.L., Kirchner, J.W. Riebe, C.S., Finkel, R.C., 2010. Mineral-specific chemical weathering rates
704 over millennial timescales: measurements at Rio Icacos, Puerto Rico. Chem. Geol. 277 (1-2), 101-114.

705 Forti, M. C., Neal, C., 1992. Hydrochemical cycles in tropical rainforests: an overview with emphasis on
706 central Amazonia. Journal of Hydrology 134(1), 103-115.

707 Fries D.M., James, R.H., Dessert, C., Bouchez, J., 2019. The response of Li and Mg isotopes to rain events
708 in a highly-weathered catchment. Chem. Geol. 519, 68-82.

709 Gaillardet J., Braud I., Hankard F., et al., 2018. OZCAR: The French Network of Critical Zone
710 Observatories. Vadose Zone Journal, 17, doi:10.2136/vzj2018.04.0067.

711 Gioda, A., Mayol-Bracero, O.L., Scatena, F.N., Weathers, K.C., Mateus, V.L., McDowell, W.H., 2013.
712 Chemical constituents in clouds and rainwater in the Puerto Rican rainforest: Potential sources and
713 seasonal drivers. Atmospheric Environment 68, 208-220.

714 Glaccum, R.A., Prospero, J.M., 1980. Saharan aerosols over the tropical north Atlantic mineralogy. Mar.
715 Geol. 37, 295–321.

716 Grousset, F. E., Biscaye, P. E., Zindler, A., Prospero, J., Chester, R., 1988. Neodymium isotopes as tracers
717 in marine sediments and aerosols: North Atlantic. Earth Planet. Sci. Lett. 87, 367-378.

718 Grousset, F. E., Rognon, P., Coudé-Gaussen, G., Pédemay, P., 1992. Origins of peri-Saharan dust deposits
719 traced by theit Nd and Sr isotopic composition. Palaeogeogr. Palaeoclimatol. Palaecoecol. 93, 203-212.

720 Grousset, F. E., Parra, M., Bory, A., Martinez, P., Bertrand, P., Shimmield, G., Ellam, R. M., 1998. Saharan
721 wind regimes traced by the Sr-Nd isotopic composition of subtropical Atlantic sediments: last glacial
722 maximum vs today. Quaternary Science Reviews 17, 395-409.

723 Guérin, A., Devauchelle, O., Robert, V., Kitou, T., Dessert, C., Quiquerez, A., Allemand, P., Lajeunesse,
724 E., 2019. Stream-discharge surges generated by groundwater flow. Geophysical Research Letters, doi:
725 10.1029/2019GL082291.

726 Hedin, L.O., Granat, L., Likens, G.E., Adri Buishand, T., Galloway, J.N., Butler, T.J., Rodhe, H., 1994. Steep
727 declines in atmospheric base cations in regions of Europe and North America. Nature 367, 351-354.

728 Heartsill-Scalley, T., Scatena, F.N., Estrada, C., W.H. McDowell, W.H., Lugo, A.E., 2007. Disturbance and
729 long-term patterns of rainfall and throughfall nutrient fluxes in a subtropical wetforest in Puerto Rico.
730 Journal of Hydrology 333, 472-485.

731 Herwitz, S.R., Muhs, D.R., Prospero, J.M., Mahan, S., Vaughn, B., 1996. Origin of Bermuda's clay-rich
732 Quaternary paleosols and their paleoclimatic significance. J. Geophys. Res.-Atmos. 101, 23389–23400.

733 Holmden, C., Bélanger, N., 2010. Ca isotope cycling in a forested ecosystem. Geochim. Cosmochim. Acta
734 74, 995-1015.

735 Jacobsen, S.B., Wasserburg, G.J., 1980. Sm-Nd isotopic evolution of chondrites. Earth Planet. Sci. Lett.
736 50 (1), 139-155.

737 Jordan, C.F, 1982. The nutrient balance of an Amazonian rain forest. Ecological Society of America 63
738 (3), 647-654.

739 Kennedy, M. J., Chadwick, O. A., Vitousek, P. M., Derry, L. A., Hendricks, D. M., 1998. Changing sources
740 of base cations during ecosystem development, Hawaiian Islands. Geology 26(11), 1015-1018.

741 Kurtz, A. C., Derry, L. A., Chadwick, O. A., 2001. Accretion of Asian dust to Hawaiian soils: isotopic,
742 elemental, and mineral mass balances. Geochim. Cosmochim. Acta 65(12), 1971-1983.

743 Liao, J. H., Wang, H. H., Tsai, C. C., & Hseu, Z. Y., 2006. Litter production, decomposition and nutrient
744 return of uplifted coral reef tropical forest. Forest ecology and management 235(1), 174-185.

745 Liu X-M., Rudnick R.L., McDonough W.F., Cummings M.L., 2013. Influence of chemical weathering on
746 the composition of the continental crust: Insights from Li and Nb isotopes in bauxite profiles developed
747 on Columbia River Basalts. Geochim. Cosmochim. Acta 115, 73-91.

748 Lloret E., C. Dessert, H. L. Buss, C. Chaduteau, S. Huon, P. Alberic, Benedetti M.F., 2016. Sources of
749 dissolved organic carbon in small volcanic mountainous tropical rivers, examples from Guadeloupe
750 (French West Indies) Geoderma 282, 129–138.

751 Mahowald, N.M., Muhs, D.R., Levis, S., Rasch, P.J., Yoshioka, M., Zender, C.S., Luo, C., 2006. Change in
752 atmospheric mineral aerosols in response to climate: last glacial period, pre-industrial, modern, and
753 doubled carbon dioxide climates. J. Geophys. Res.-Atmos. 111 (D10).

754 McClintock, M.A., Brocard, G., Willenbring, J., Tamaya, C., Porder, S., Pett-Ridge, J.C., 2015. Spatial
755 variability of African dust in soils in a montane tropical landscape in Puerto Rico. Chem. Geol. 412, 69-
756 81.

757 McDowell, W.H., 1998. Internal nutrient fluxes in a Puerto Rican rain forest. Journal of Tropical Ecology
758 14, 521-536.

759 Meynadier, L., Gorge, C., Birck, J.-L., Allègre, C.J., 2006. Automated separation of Sr from natural water
760 samples or carbonate rocks by high performance ion chromatography. Chem. Geol. 227, 26-36.

761 Moreno, T., Querol, X., Castillo, S., Alastuey, A., Cuevas, E., Herrmann, L., Mounkaila, M.,Elvira, J.,
762 Gibbons, W., 2006. Geochemical variations in aeolian mineral particles from the Sahara–Sahel Dust
763 Corridor. Chemosphere 65, 261–270.

764 Muhs, D.R., Bush, C.A., Stewart, K.C., Rowland, T.R., Crittenden, R.C., 1990. Geochemical evidence of
765 Saharan dust parent material for soils developed on Quaternary limestones of Caribbean and Western
766 Atlantic islands. Quaternary Research 33, 157-177.

767 Muhs, D.R., Budahn, J., Prospero, J.M., Carey, S.N., 2007. Geochemical evidence for African dust inputs
768 to soils of western Atlantic islands: Barbados, the Bahamas and Florida. J. Geophys. Res. 112, F02009.
769 Okin, G.S., Mahowald, N., Chadwick, O.A., Artaxo, P., 2004. Impact of desert dust on the
770 biogeochemistry of phosphorus in terrestrial ecosystems. Glob. Biogeochem. Cycles 18, GB2005.

771 Opfergelt, S., Georg, R.B., Delvaux, B., Cabidoche, Y.M., Burton, K.M., Halliday, A.N., 2012. Mechanisms
772 of magnesium isotope fractionation in volcanic soil weathering sequences, Guadeloupe. Earth Planet.
773 Sci. Lett. 341–344, 176–185.

774 OVSG-IPGP Website. Volcano and seismic activity bulletin of La Soufrière of Guadeloupe.
775 http://www.ipgp.fr/fr/ovsg/observatoire-volcanologique-sismologique-de-guadeloupe.

776 Pett-Ridge, J.C., 2009. Contributions of dust phosphorus cycling in tropical forests of the Luquillo
777 Mountains, Puerto Rico. Biogeochemistry 94, 63-80.

778 Pett-Ridge, J.C., Derry, L.A., Barrows, J.K., 2009a. Ca/Sr and $^{87}Sr/^{86}Sr$ ratios as tracers of Ca and Sr cycling
779 in the Rio Icacos watershed, Luquillo Mountains, Puerto Rico. Chem. Geol. 267(1), 32-45.

780 Pett-Ridge, J.C., Derry, L.A., Kurtz A.C., 2009b. Sr isotopes as a tracer of weathering processes and dust
781 inputs in a tropical granitoid watershed, Luquillo Mountains, Puerto Rico. Geochim. Cosmochim. Acta
782 73, 25-43.

783 Porder, S., Clark, D.A., Vitouseck, P.M., 2006. Persistence of rock-derived nutrients in the wet tropical
784 forests of La Selva, Costa Rica. Ecology 87, 594-602.

785 Poszwa, A., Dambrine, E., Ferry, B., Pollier B., Loubet, M., 2002. Do deep tree roots provide nutrients
786 to the tropical rainforest? Biogeochemistry 60, 97-118.

787 Proctor, J., 1987. Nutrient cycling in primary and old secondary rainforests. Applied Geography 7, 135-
788 152.

789 Prospero, J.M., 1999. Long-term measurements of the transport of African mineral dust to the
790 southeastern United States: implications for regional air quality. Journal of Geophysical Research 104,
791 15917–15927.

792 Prospero, J.M., Bonatti, E., Schubert, C., Carlson, T.N., 1970. Dust in Caribbean atmosphere traced to
793 an African dust storm. Earth Planet. Sci. Lett. 9, 287–290.

794 Prospero, J.M., Glaccum, R.A., Nees, R.T., 1981. Atmospheric transport of soil dust from Africa to South
795 America. Nature 289, 570–572.

796 Schlesinger, W.H., 1997. Biogeochemistry: an analysis of global change. Academic Press, San Diego,
797 California, USA.

798 Richard, P., Shimizu, N., Allègre, C.J., 1976. 143Nd/146Nd, a natural tracer: an application tooceanic
799 basalts. Earth Planet. Sci. Lett. 31 (2), 269–278.

800 Riotte, J., Marechal, J. C., Audry, S., Kumar, C., Bedimo, J. B., Ruiz, L., ... & Braun, J. J., 2014. Vegetation
801 impact on stream chemical fluxes: Mule Hole watershed (South India). Geochim. Cosmochim. Acta 145,
802 116-138.

803 Rognon, P., Coudé-Gaussen, G., Revel, M., Grousset, F. E., Pédemay, P., 1996. Holocene Saharan dust
804 deposition on the Cape Verde Islands: sedimentological and Nd-Sr isotopic evidence. Sedimentology
805 43, 359-366.

806 Rousteau, A., 1996. Structures, flores, dynamiques: réponses des forêts pluviales des Petites Antilles
807 aux milieux montagnards. In: Guillaumet, J.L., Belin, M., Puig, H. (Eds.), Phytogéographie Tropicale:
808 Réalités et Perspectives. ORSTOM, Paris, pp. 307–321.

809 Rousteau, A., Dessert, C., Dulormne, M., 2014. Bilan des travaux réalisés dans le cadre du projet
810 "Vulnérabilité des écosystèmes insulaires guadeloupéens aux changements climatiques". Région
811 Guadeloupe funding.

812 Rousteau, A., Portecop, J., Rollet, B., 1994. Carte écologique de la Guadeloupe. Université Antilles-
813 Guyane, ONF, Conseil Général, Parc National de la Guadeloupe, Guadeloupe.

814 Samper, A., Quidelleur, X., Lahitte, P., Mollex, D., 2007. Timing of effusive volcanism and collapse events
815 within an oceanic arc island: Basse-Terre, Guadeloupe archipelago (Lesser Antilles Arc). Earth Planet.
816 Sci. Lett. 258, 175–191.

817 Schuessler, J.A., von Blanckenburg, F., Bouchez, J., Uhlig, D., Hewawasam, T., 2018. Nutrient cycling in
818 a tropical montane rainforest under a supply-limited weathering regime traced by elemental mass
819 balances and Mg stable isotopes. Chem. Geol. 497, 74-87.

820 Soderberg, K., Compton, J.S., 2007. Dust as a Nutrient Source for Fynbos Ecosystems, South Africa.
821 Ecosystems 10, 550-561.

822 Stewart, B. W., Capo, R. C., Chadwick, O. A., 2001. Effects of rainfall on weathering rate, base cation
823 provenance, and Sr isotope composition of Hawaiian soils. Geochim. Cosmochim. Acta 65(7), 1087-
824 1099.

825 Stille, P., Schmitt, A.-D., Labolle, F., Pierret, M.-C., Gangloff, S., Cobert, F., Lucot, E., Guéguen, F., Brioschi,
826 L., Steinmann, M., Chabaux, F., 2012. The suitability of annual tree growth rings as environmental

archives: Evidence from Sr, Nd, Pb and Ca isotopes in spruce growth rings from the Strengbach watershed. C. R. Geoscience 344, 297-311.

Taylor, S.R. and McLennan, S.M., 1985. The Continental Crust: Its Composition and Evolution. Blackwell, Oxford, 1-312.

Turner, B. F., Stallard, R. F., & Brantley, S. L., 2003. Investigation of in situ weathering of quartz diorite bedrock in the Rio Icacos basin, Luquillo Experimental Forest, Puerto Rico. Chem. Geol. 202, 313-341.

Van Laere, G., Gall, Y. and Rousteau, A., 2016. The forest Ecosystems Observatory in Guadeloupe (FWI). Caribbean Naturalist, Special Issue n°1: 108-115.

Vitousek, P. M., Sanford, R. L., 1986. Nutrient cycling in moist tropical forest. Annu. Rev. Ecol. Syst. 17, 137-167.

Weaver, P.L., Murphy, P.G., 1990. Forest structure and productivity in Puerto Rico's Luquillo Mountains. Biotropica 22 (1), 69–82.

Whipkey, C. E., Capo, R. C., Chadwick, O. A., Stewart, B. W., 2000. The importance of sea spray to the cation budget of a coastal Hawaiian soil: a strontium isotope approach. Chem. Geol. 168(1), 37-48.

White, W.M., Dupré, B., 1986. Sediment subduction and magma genesis in the Lesser Antilles: isotopic and trace element constraints. J. Geophys. Res. 91, 5927–5941.

White, W.M., Patchett, J., 1984. Hf-Nd-Sr isotopes and incompatible element abundances in island arcs; implications for magma origins and crust-mantle evolution. Earth and Planetary Science Letters 67, 167-185.

Wilcke, W., Velescu, A., Leimer, S., Bigalke, M., Boy, J., Valarezo, C., 2017. Biological versus geochemical control and environmental change drivers of the base metal budgets of a tropical montane forest in Ecuador during 15 years. Biogeochemistry 136, 167-189.

Xu, Y., Losno, R., Dessert, C., Monna, F., Robert, V., Chane-Teng, J., 2017. Compositional analysis of Saharan dust input to Guadeloupe (FWI). Goldschmidt Conference, Paris, 2017 August 13-18, 16d/3045.

Yu, H., Chin, M., Yuan, T., Bian, H., Remer, L.A., Prospero, J.M., Omar, A., Winker, D., Yang, Y., Zhang, Y., Zhang, Z., Zhao, C., 2015. The fertilizing role of African dust in the Amazon rainforest: A first multiyear assessment based on data from Cloud-Aerosol Lidar and Infrared Pathfinder Satellite Observations. Geophys. Res. Lett. 42, 1984-1991.

Zahibo, N., Pelinovsky, E., Talipova, T., Rabinovich, A., Kurkin, A., Nikolkina, I., 2007. Statistical analysis of cyclone hazard for Guadeloupe, Lesser Antilles. Atmos. Res. 84, 13-29.

858 Figure caption

859 Fig. 1. The Quiock Creek catchment (16°17'N, 61°70'W) in the Guadeloupe National Park. The MF rain
860 gauge is located in a clearing, on the roof of the “Maison de la Forêt”, and the OVSG rain gauge is
861 located on the roof of the observatory. The soil profile was sampled during lysimeter installation (see
862 Buss et al., 2010).

863 Fig. 2. Sr isotopic composition of dissolved and solid samples collected in the Quiock Creek catchment.
864 Sea salt Sr isotopic ratio = 0.70917 (Dia et al., 1992); volcanic rock = 0.7038 (this study); Saharan dust
865 = 0.7187 (this study).

866 Fig. 3. Molar ratios (µmol/µmol ratios, except for the Sr/Cl ratio expressed in nmol/µmol) of dissolved
867 load in the different compartments of the Quiock Creek catchment. RF: rainfall, TF: throughfall, SS: soil
868 solution (above and below 91 cm depth), QC: Quiock Creek, SW: seawater/sea salt.

869 Fig. 4. Soil profiles. Quartz + feldspar content (from Buss et al., 2010), mass transfer coefficient (τ) for
870 Sr in soil samples relative to bedrock, and isotopic signature of Sr and Nd. τ is calculated considering Ti
871 to be immobile and illustrates the extreme depletion of Sr in the soil compared to unweathered rock
872 (values closed to -1).

873 Fig. 5. Cation fluxes in the Quiock Creek catchment expressed in kg/ha/yr. $F_{SW}$ is the sea salt flux, $F_{SD}$
874 the Saharan dust leaching flux, $F_{RF}$ the rainfall flux, $F_{TF}$ the throughfall flux, $F_{LF}$ the litter fall flux, $F_{EX}$
875 the leaf excretion flux and $F_{QC}$ the Quiock Creek flux.

876 Fig. 6. Sr mass transfer coefficient as a function of Sr isotopic ratio in soil samples. Sea salt Sr isotopic
877 ratio = 0.70917 (Dia et al., 1992); volcanic rock = 0.7038 (this study); Saharan dust = 0.7187 (this study).
878 Samples enriched in quartz-feldspar are symbolized by white square.

879 Fig. 7. Two-component mixing diagram of εNd vs. Sr isotopic ratio in soil samples. Horizon depths (cm)
880 are added and samples enriched in quartz-feldspar are symbolized by white squares. The solid lines

represent different mixing curves between a bedrock (fresh and depleted) end-member and a “Saharan dust” end-member. The mixing proportions are expressed in % of dust Sr. The black dotted curve represents a mixture of fresh rock ($^{87}Sr/^{86}Sr$ = 0.7038, εNd = 4.8, Sr/Nd = 17.9) and dust ($^{87}Sr/^{86}Sr$ = 0.7187, εNd = -11.5, Sr/Nd = 3.4). The other curves show a mixture between of depleted rock ($^{87}Sr/^{86}Sr$ = 0.7038, εNd = 4.8, Sr/Nd varying from 10 to 0.1 for the most depleted rock) and dust. The samples are explained by a mixture of Saharan dust and depleted rock. The soil horizons enriched in quartz-feldspar are strongly influenced by dust (20 to 65% of dust Sr). The near-surface horizon (first 30 cm) is the most impacted by dust and can be explained by the mixing of dust with moderately depleted rock. This emphasizes the contemporary, or very recent, deposition of both Saharan dust and volcanic ash in Guadeloupe (recent volcanic activity of nearby Montserrat). The deeper quartz-feldspar horizons are paleo-surfaces of dust deposits interspersed with volcanic deposits. With time, andesitic and dust-derived Sr has been leached extensively and the sea salt Sr signature dominates today in the entire profile.

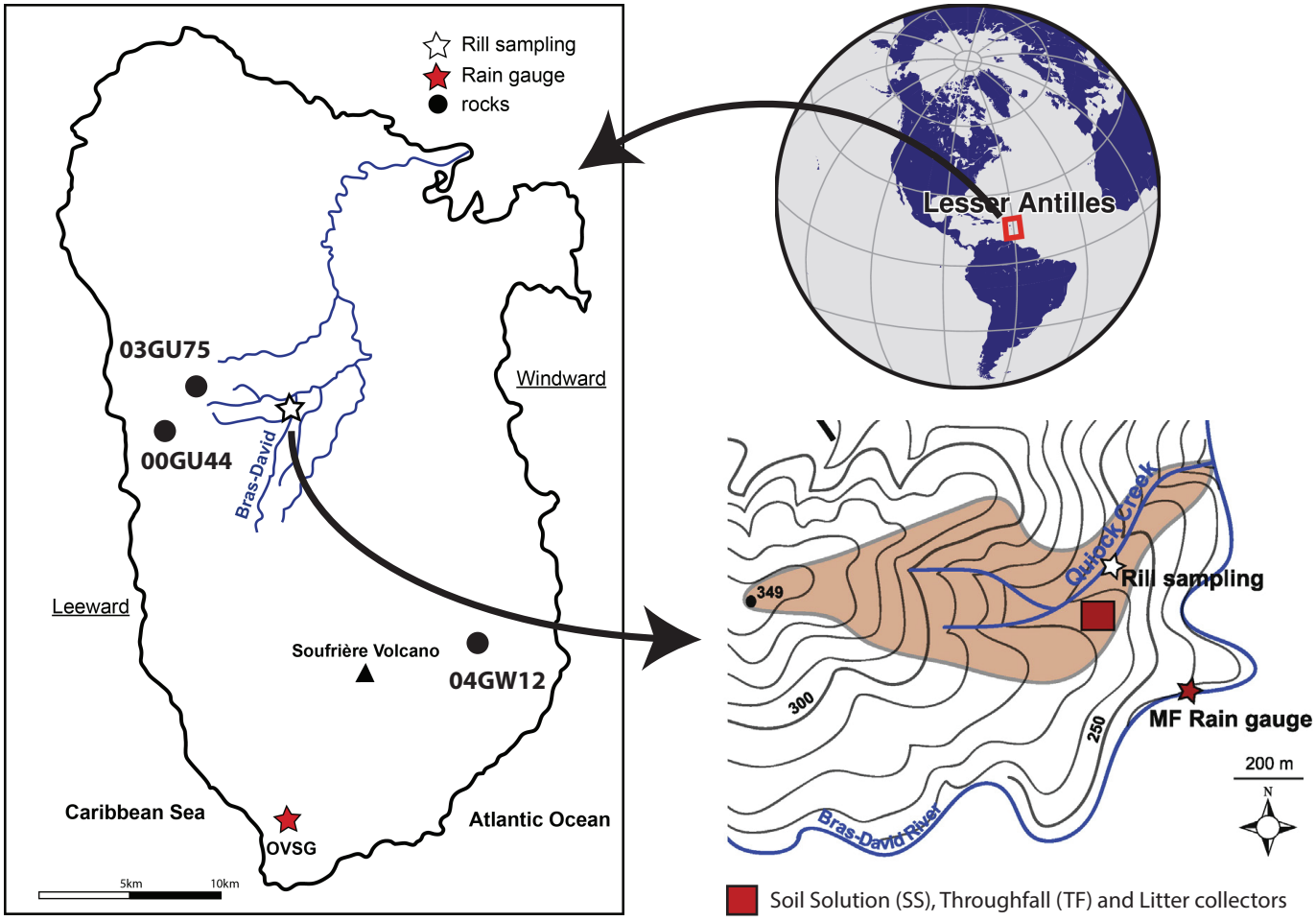
Rill sampling
Rain gauge
rocks
03GU75
00GU44
Bras-David
Windward
Leeward
Soufrière Volcano
04GW12
Caribbean Sea
Atlantic Ocean
OVSG
5km
10km
Lesser Antilles
Quiock Creek
Rill sampling
MF Rain gauge
349
300
250
200 m
N
Bras-David River
Soil Solution (SS), Throughfall (TF) and Litter collectors

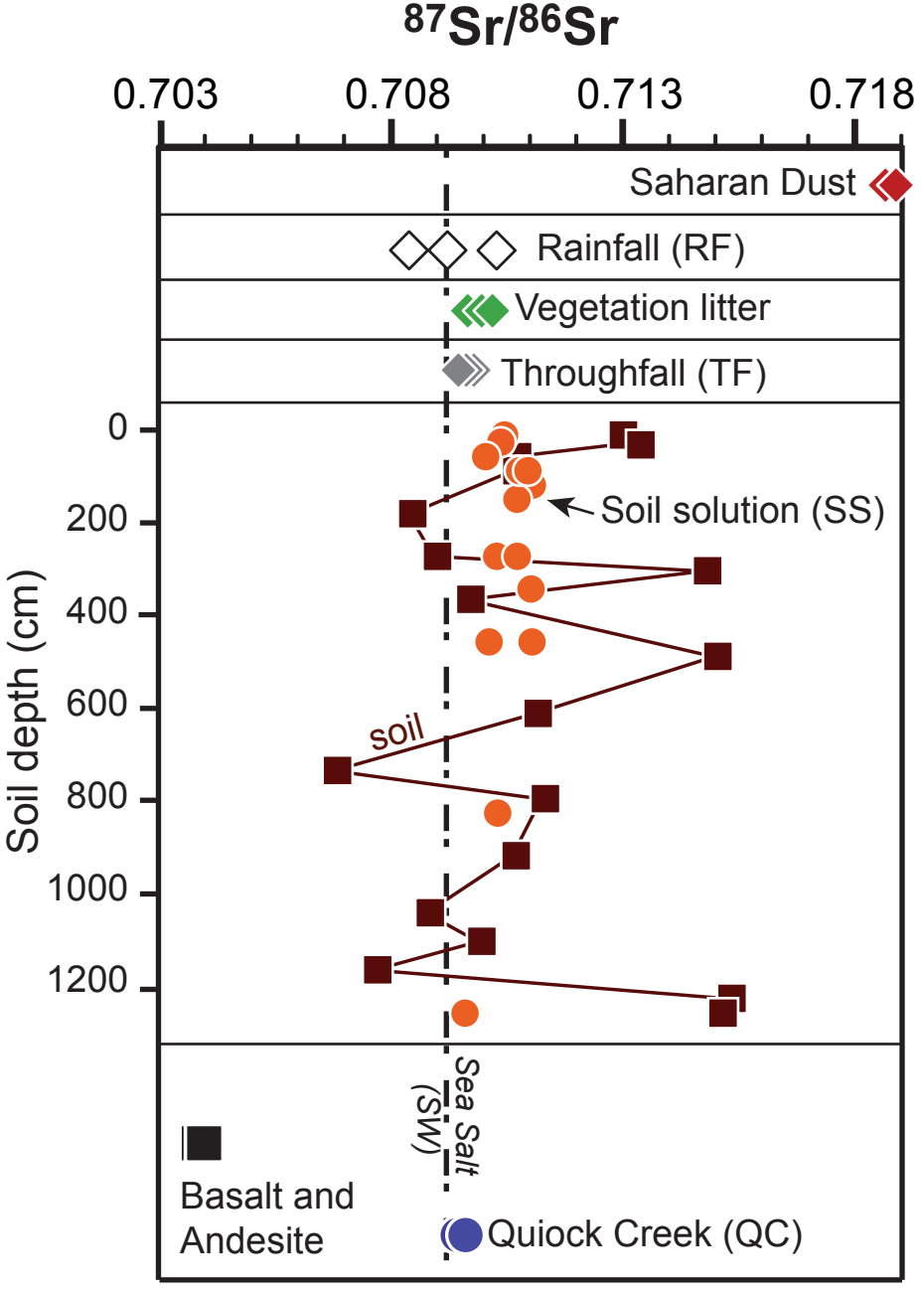
87Sr/86Sr
0.703
0.708
0.713
0.718
Saharan Dust
Rainfall (RF)
Vegetation litter
Throughfall (TF)
Soil solution (SS)
soil
Soil depth (cm)
0
200
400
600
800
1000
1200
Sea Salt (SW)
Basalt and Andesite
Quiock Creek (QC)

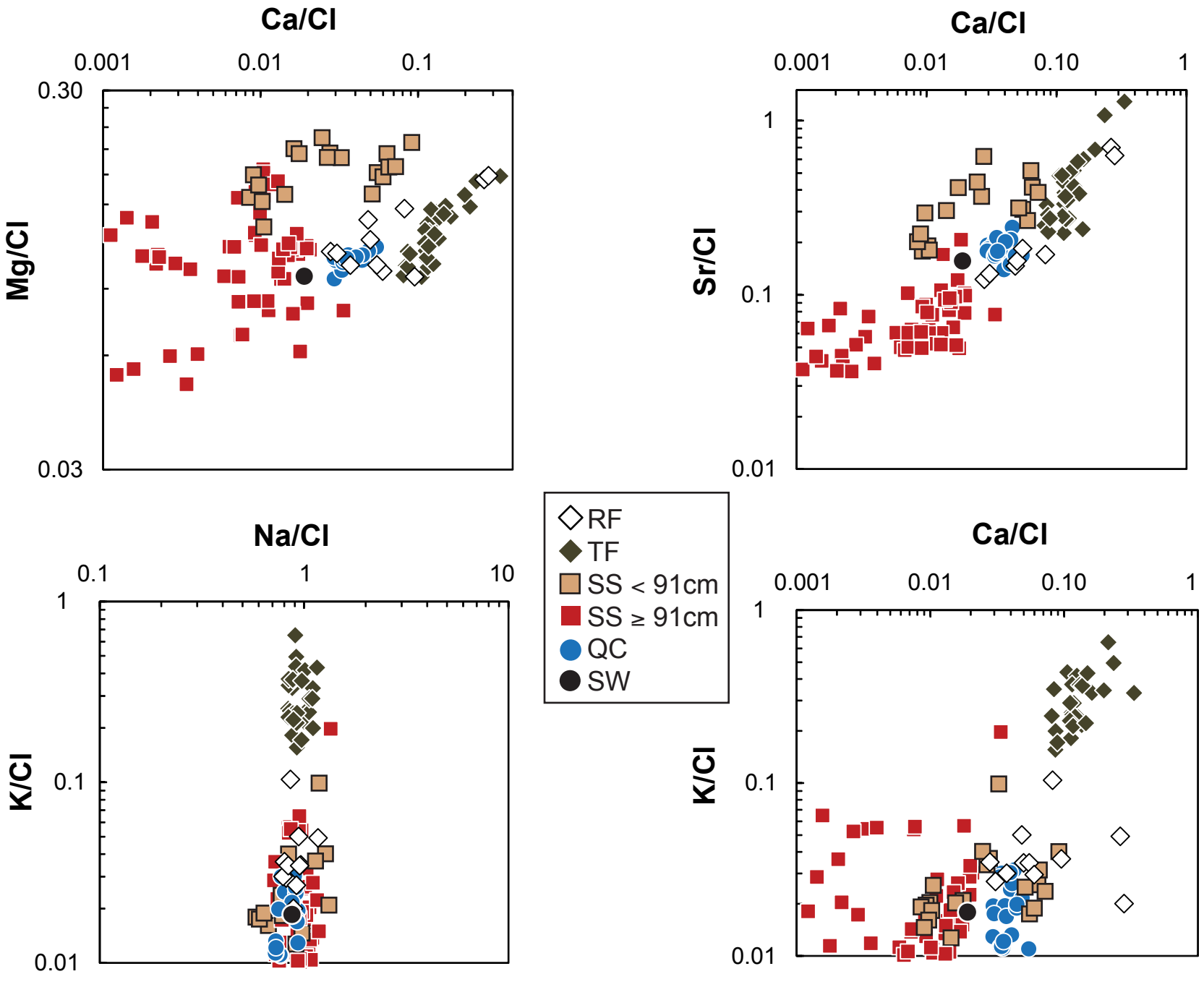
Ca/Cl
0.001
0.01
0.1
0.30
0.03
Mg/Cl
Ca/Cl
0.001
0.01
0.10
1
1
0.1
0.01
Sr/Cl
Na/Cl
0.1
1
10
1
0.1
0.01
K/Cl
RF
TF
SS < 91cm
SS ≥ 91cm
QC
SW
Ca/Cl
0.001
0.01
0.10
1
1
0.1
0.01
K/Cl

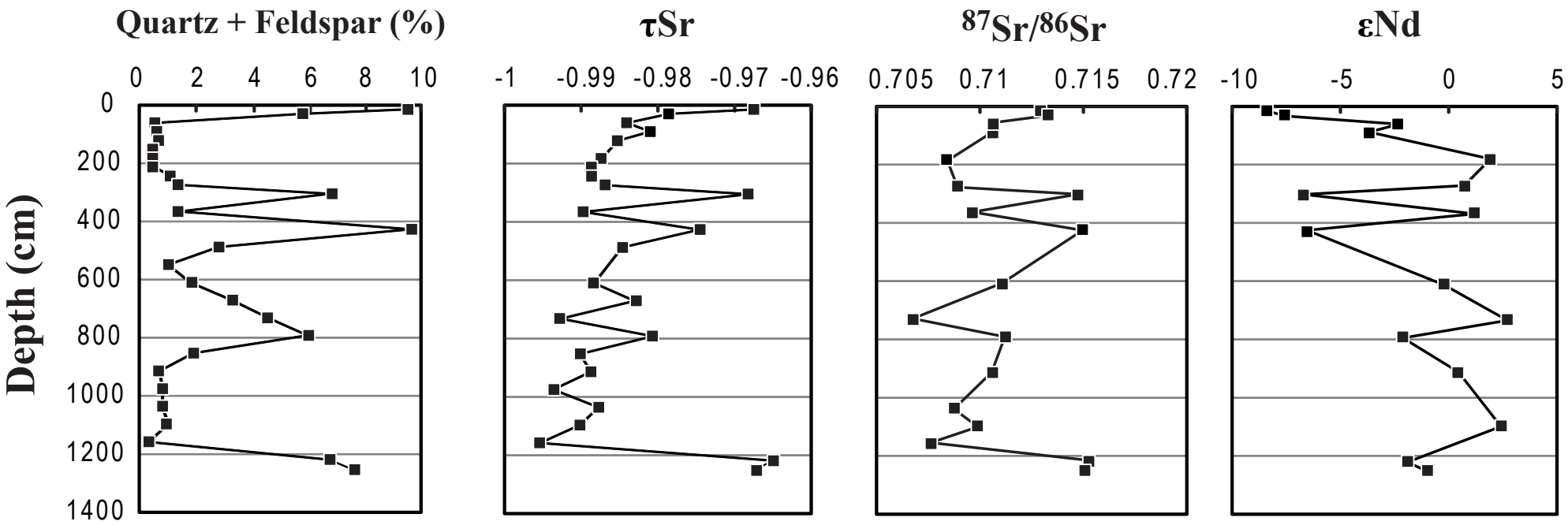
Quartz + Feldspar (%)
τSr
87Sr/86Sr
εNd
Depth (cm)
0
200
400
600
800
1000
1200
1400
0 2 4 6 8 10
-1 -0.99 -0.98 -0.97 -0.96
0.705 0.71 0.715 0.72
-10 -5 0 5

## Mg

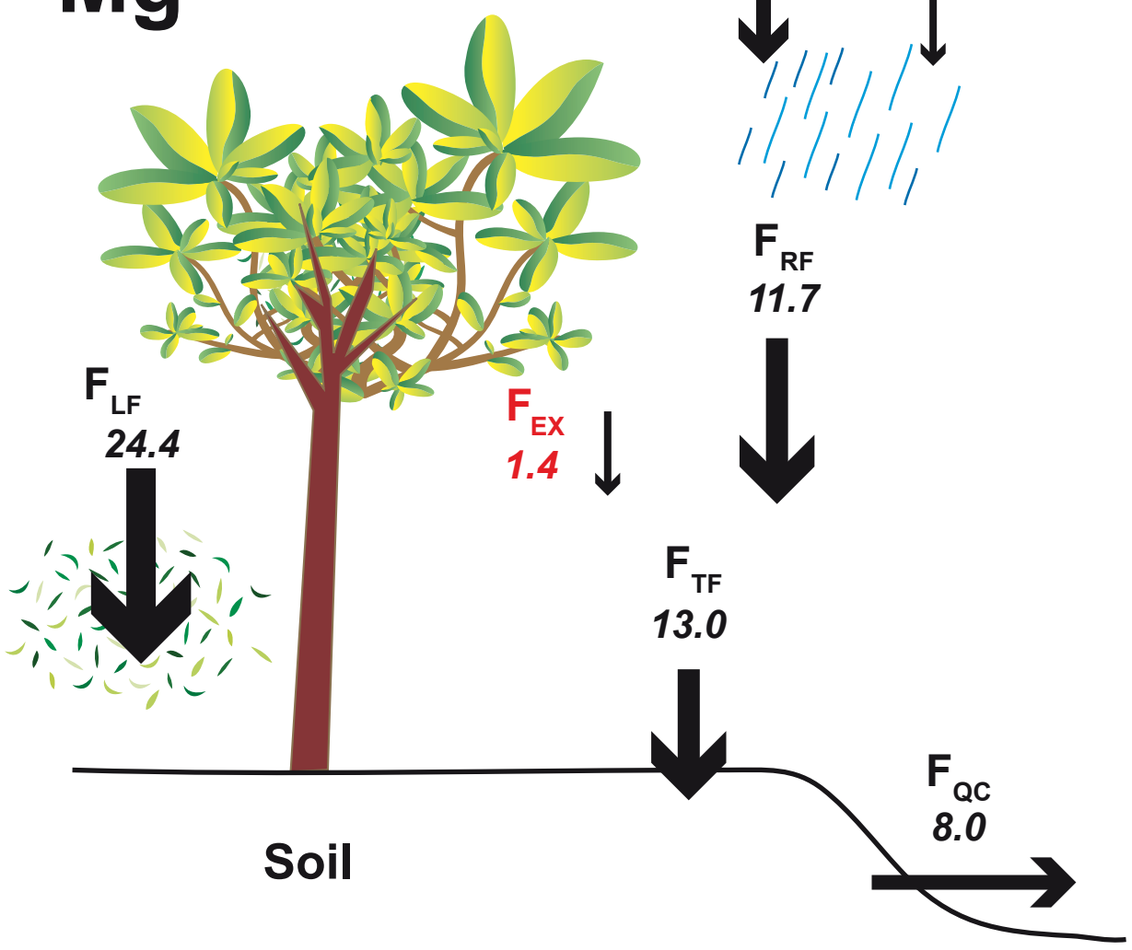
F SW
9.6
F SD
2.1
F RF
11.7
F LF
24.4
F EX
1.4
F TF
13.0
F QC
8.0
Soil

## Na

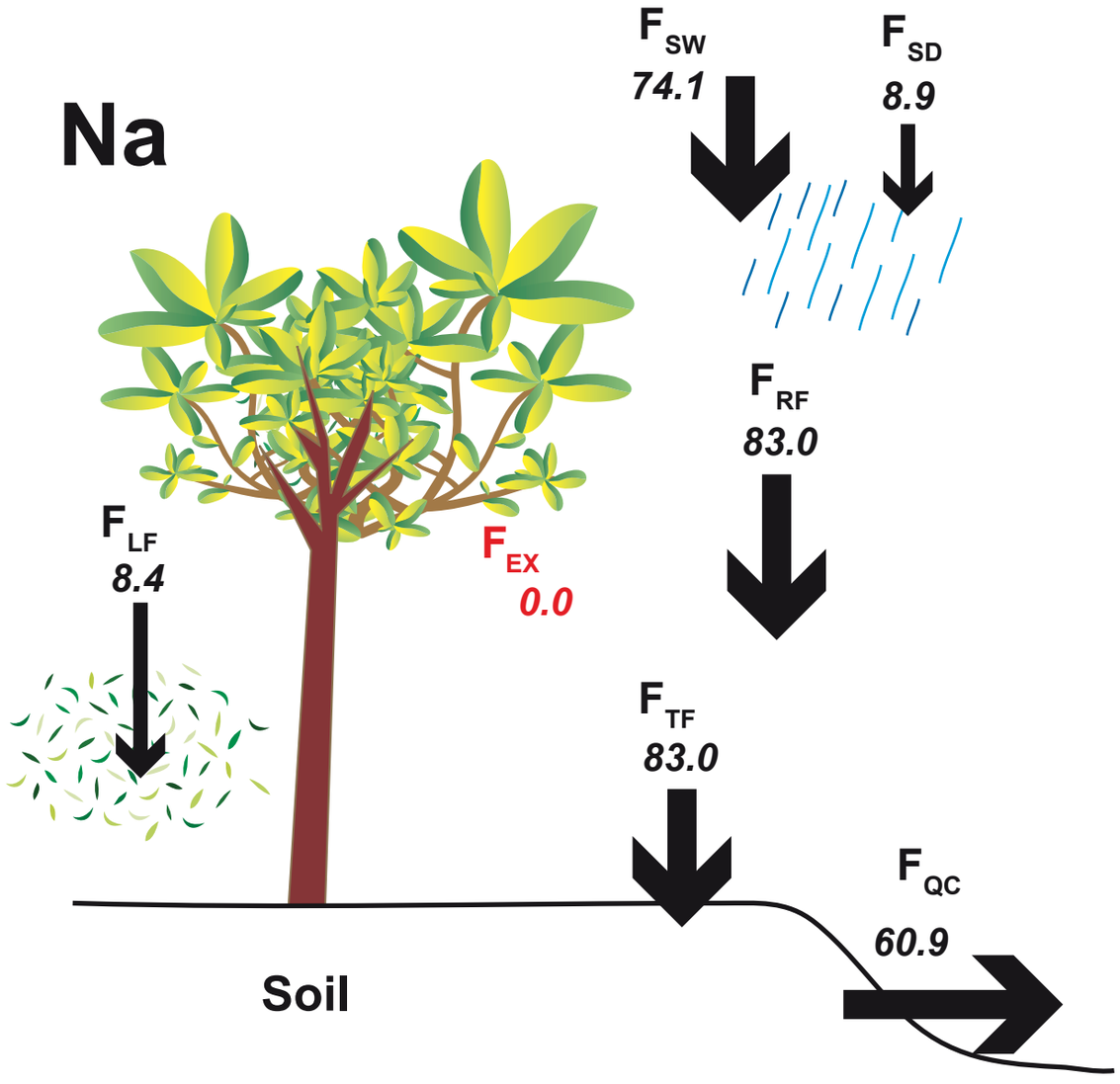
F SW
74.1
F SD
8.9
F RF
83.0
F LF
8.4
F EX
0.0
F TF
83.0
F QC
60.9
Soil

## Ca

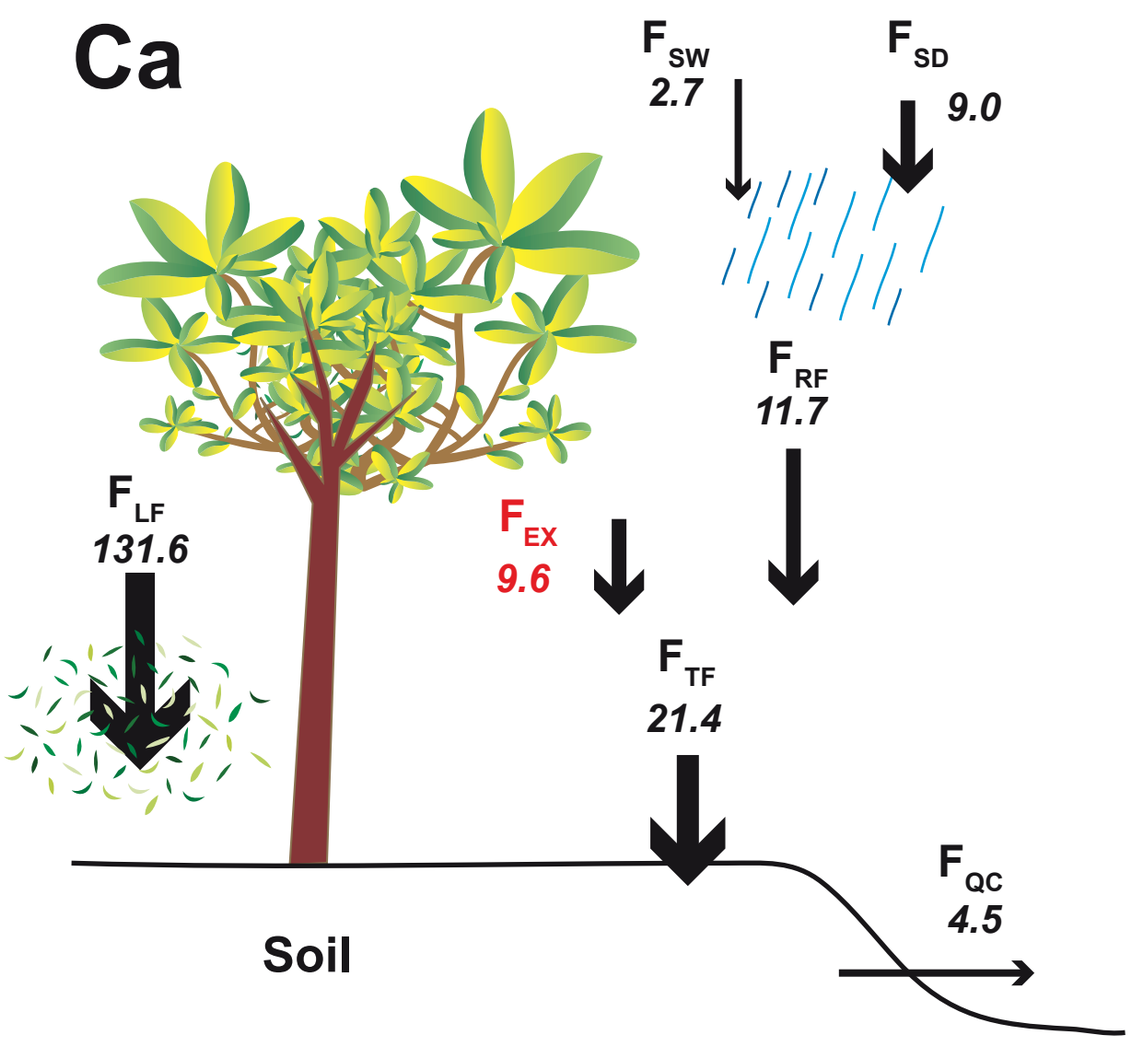
F SW
2.7
F SD
9.0
F RF
11.7
F LF
131.6
F EX
9.6
F TF
21.4
F QC
4.5
Soil

## K

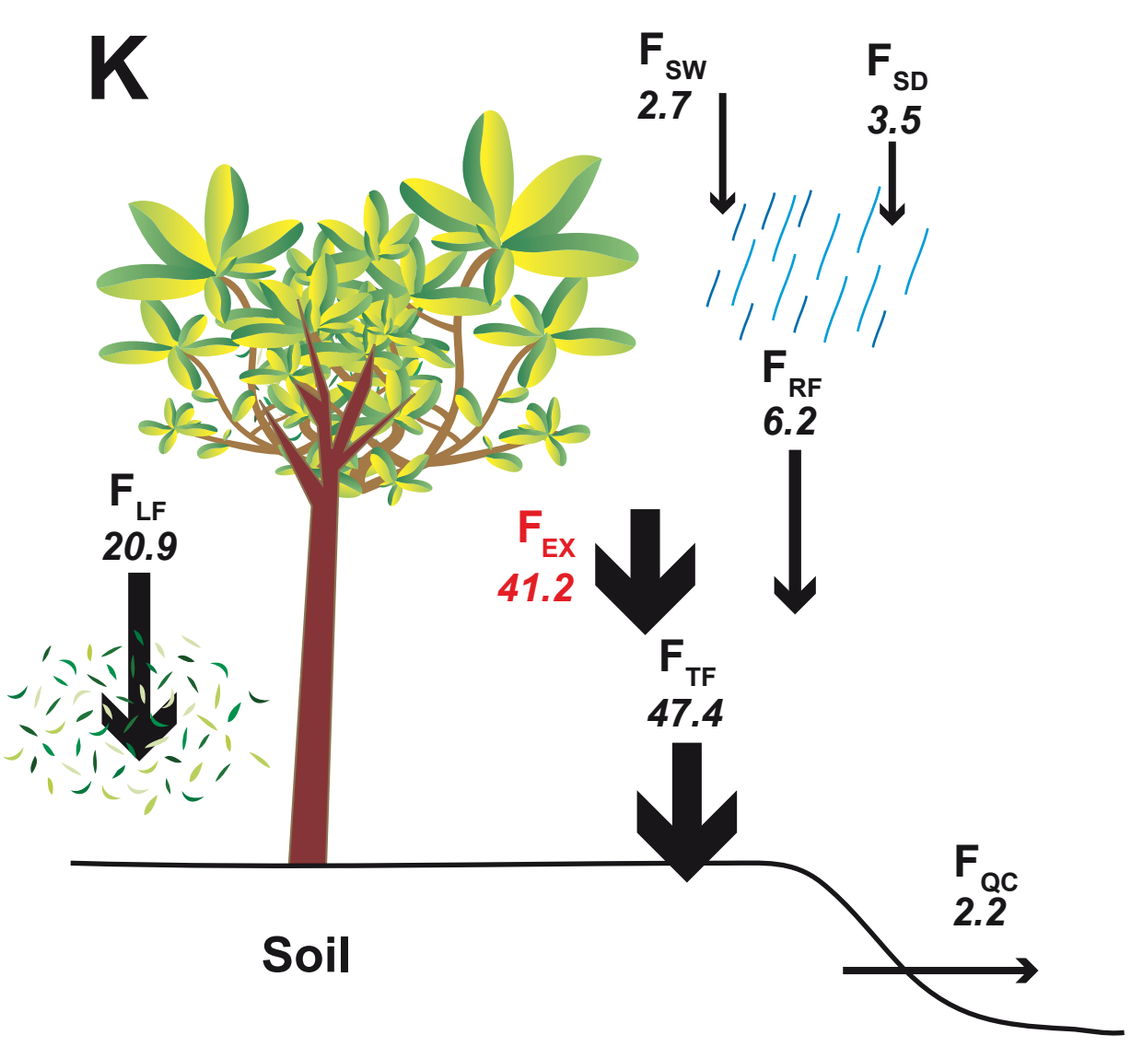
F SW
2.7
F SD
3.5
F RF
6.2
F LF
20.9
F EX
41.2
F TF
47.4
F QC
2.2
Soil

## Sr

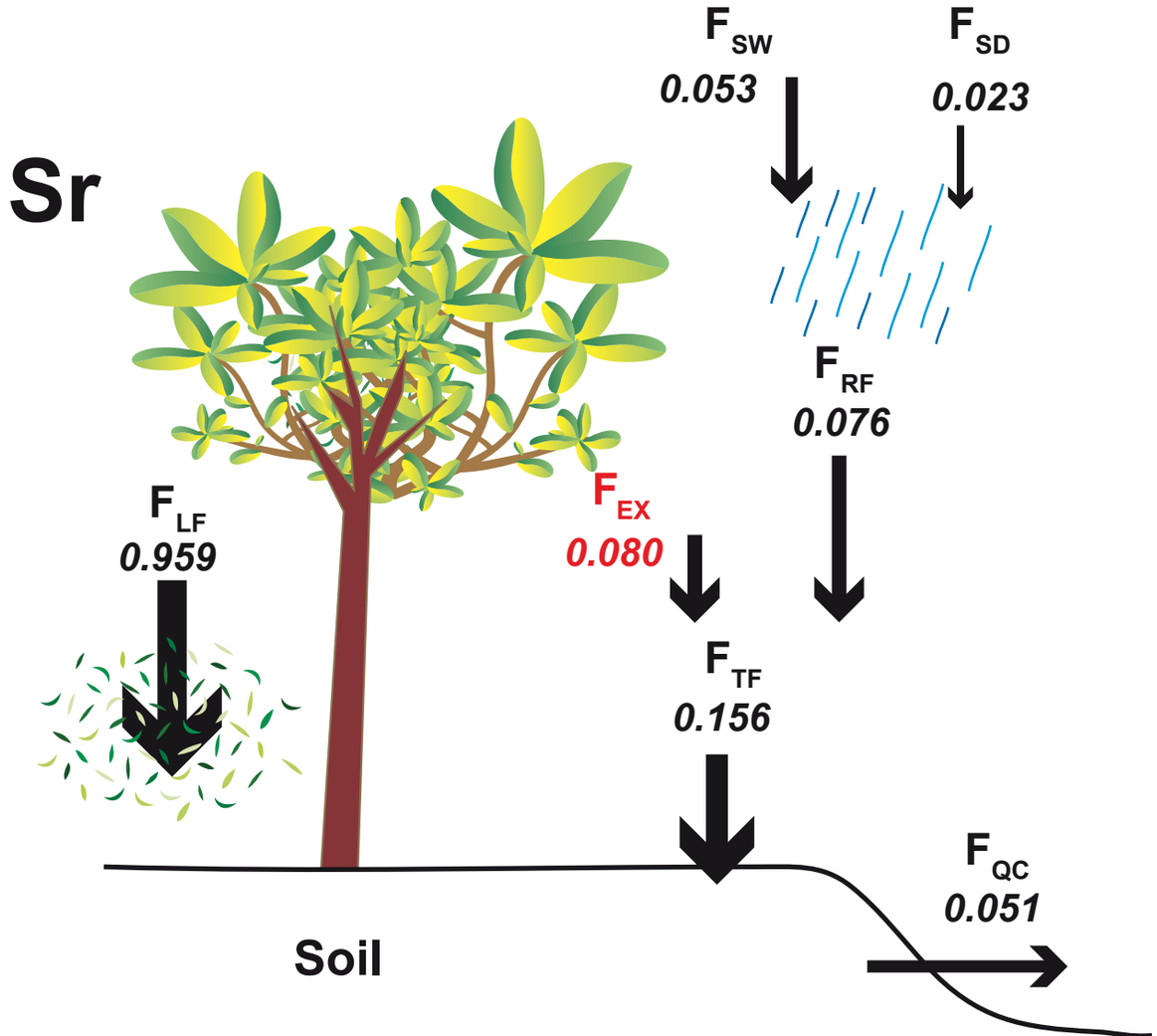
F SW
0.053
F SD
0.023
F RF
0.076
F LF
0.959
F EX
0.080
F TF
0.156
F QC
0.051
Soil

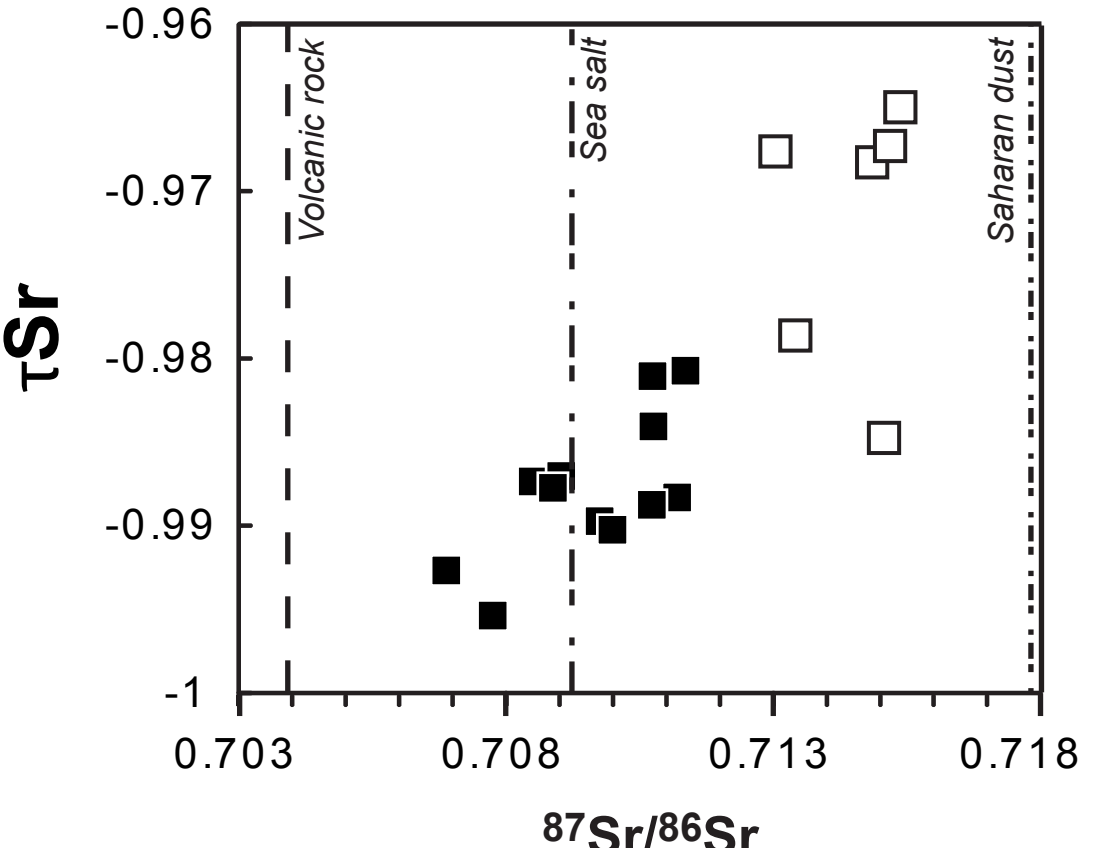
-0.96
-0.97
-0.98
-0.99
-1
τSr
Volcanic rock
Sea salt
Saharan dust
0.703
0.708
0.713
0.718
87Sr/86Sr

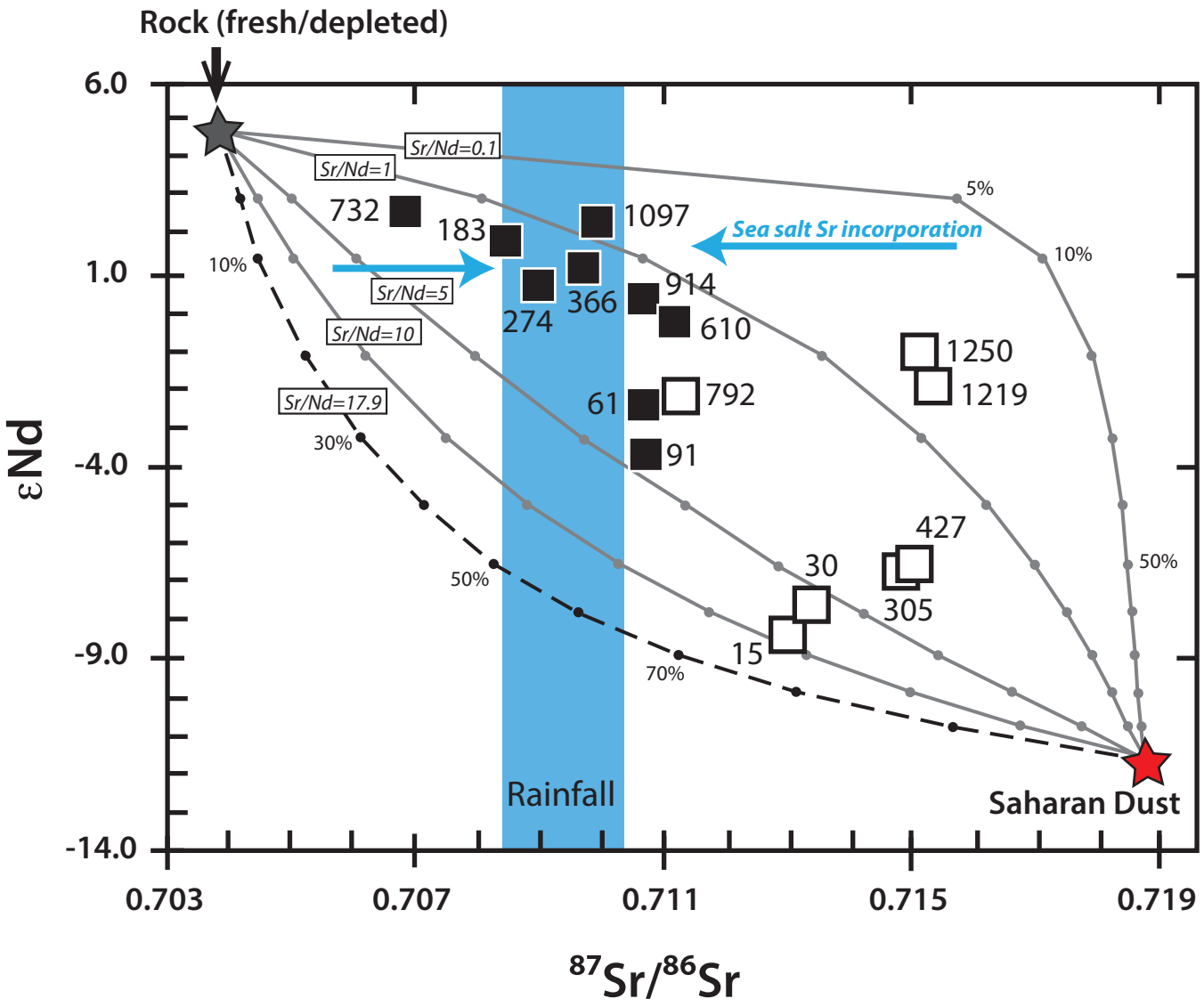
Rock (fresh/depleted)
6.0
1.0
-4.0
-9.0
-14.0
εNd
0.703
0.707
0.711
0.715
0.719
87Sr/86Sr
Sr/Nd=0.1
Sr/Nd=1
Sr/Nd=5
Sr/Nd=10
Sr/Nd=17.9
Sea salt Sr incorporation
Rainfall
Saharan Dust
5%
10%
30%
50%
70%
732
183
1097
914
610
366
274
1250
1219
792
61
91
427
30
305
15

Tables_Results

Table 1: Major element concentrations are from Clergue et al. (2015). Sr concentrations and Sr isotopic signature in water samples are new data.

| **Sample name** | **Date** dd/mm/yy | **pH** | **Na** µmol/L | **Cl** µmol/L | **Ca** µmol/L | **Mg** µmol/L | **K** µmol/L | **Sr** µmol/L | **$^{87}Sr/^{86}Sr$** |
|---|---|---|---|---|---|---|---|---|---|
| *Rainfall (RF)* | | | | | | | | | |
| RF-OVSG | 20/03/13 | 4.8 | 82 | 85 | 2 | 10 | 3 | 0.010 | 0.70918 |
| RF-OVSG | 04/04/13 | 5.1 | 76 | 88 | 7 | 13 | 9 | 0.015 | 0.70841 |
| RF-OVSG | 15/07/13 | nd[a] | 96 | nd | 7 | 14 | 5 | 0.034 | 0.71029 |
| *Throughfall (TF)* | | | | | | | | | |
| TF collector n°2 | 21/11/11 | nd | 25 | 27 | 6 | 4 | 18 | 0.121 | 0.70965 |
| TF collector n°1 | 10/08/12 | 6.1 | 81 | 92 | 15 | 13 | 31 | 0.056 | 0.70978 |
| TF collector n°3 | 21/03/13 | 5.6 | 71 | 64 | 6 | 7 | 13 | 0.015 | 0.70953 |
| TF collector n°1 | 03/04/13 | nd | 155 | 168 | 14 | 19 | 26 | 0.048 | 0.70969 |
| TF collector n°3 | 03/04/13 | nd | 154 | 158 | 14 | 18 | 27 | 0.043 | 0.70972 |
| TF collector n°1 | 25/06/13 | 5.6 | 117 | 132 | 17 | 17 | 32 | 0.067 | 0.70968 |
| *Soil solution (SS)[b]* | | | | | | | | | |
| GBD2_91 | 26/10/12 | 5.1 | 226 | 211 | 3 | 21 | 3 | 0.022 | 0.71070 |
| GBD2_122 | 26/10/12 | 4.9 | 171 | 145 | 2 | 16 | 2 | 0.009 | 0.71097 |
| GBD2_152 | 26/10/12 | 4.6 | 153 | 141 | 1 | 22 | 1 | 0.008 | 0.71063 |
| GBD2_274 | 26/10/12 | 4.6 | 209 | 241 | 4 | 28 | 5 | 0.022 | 0.71020 |
| GBD2_344 | 26/10/12 | 4.5 | 207 | 244 | 0 | 30 | 2 | 0.009 | 0.71094 |
| GBD2_457 | 26/10/12 | 4.5 | 194 | 168 | 2 | 14 | 4 | 0.013 | 0.71004 |
| GBD2_15 | 28/06/13 | nd | 118 | 130 | 2 | 21 | 2 | 0.039 | 0.71037 |
| GBD2_30 | 28/06/13 | 5.4 | 147 | 150 | 1 | 27 | 2 | 0.034 | 0.71029 |
| GBD2_61 | 28/06/13 | 4.8 | 126 | 163 | 12 | 31 | 4 | 0.063 | 0.70996 |
| GBD2_91 | 28/06/13 | 5.3 | 194 | 207 | 3 | 25 | 2 | 0.020 | 0.71087 |
| GBD2_274 | 28/06/13 | 4.7 | 161 | 221 | 2 | 26 | 2 | 0.017 | 0.71064 |
| GBD2_457 | 28/06/13 | 5.4 | 159 | 167 | 2 | 14 | 3 | 0.010 | 0.71097 |
| GBD2_823 | 28/06/13 | nd | 210 | 243 | 1 | 15 | 13 | 0.010 | 0.71022 |
| *Quiock Creek* | | | | | | | | | |
| QC | 23/04/12 | nd | 184 | 229 | 11 | 25 | 6 | 0.056 | 0.70939 |
| QC | 03/08/12 | nd | 248 | 271 | 9 | 29 | 5 | 0.052 | 0.70922 |
| QC | 26/10/12 | 4.7 | 254 | 271 | 8 | 30 | 4 | 0.048 | 0.70933 |
| QC | 21/03/13 | 4.8 | 211 | 274 | 15 | 32 | 3 | 0.046 | 0.70928 |

[a] nd=not determined.

[b] For soil solution sample names GBD2_X, X=depth in cm.

Table 2: Range of concentration in the different compartments (mean value/median value) from Clergue et al. (2015).

| | K (µmol/L) | Na (µmol/L) | Mg (µmol/L) | Ca (µmol/L) | Cl (µmol/L) |
|---|---|---|---|---|---|
| RF* (n=13) | 1 – 9 (4/3) | 41 – 165 (89/79) | 1 – 22 (12/11) | 1 – 15 (7/7) | 49 – 167 (92/85) |
| TF (n=48) | 10 – 108 (39/32) | 17 – 264 (117/102) | 3 – 40 (17/17) | 3 – 36 (17/16) | 23 – 264 (125/99) |
| SS (n=75) | 1 – 39 (5/3) | 112 – 266 (179/182) | 11 – 58 (24/25) | 0.3 – 14 (3/2) | 85 – 345 (199/203) |
| QC (n=57) | 3 – 12 (5/5) | 184 – 282 (234/239) | 24 – 35 (29/29) | 7 – 15 (10/10) | 229 – 315 (272/274) |

*: MF + OVSG rainfall.

Table 3: Chemical and isotopic (Sr and Nd) composition of soil, rock, Saharan dust and vegetation samples. Some Nd isotopic composition of soils (highlighted) and Ca, K, Mg, Na, Ti concentrations are from Clergue et al. (2015).

| **Sample name** | **Ca** ppm | **K** ppm | **Mg** ppm | **Na** ppm | **Ti** ppm | **Sr** ppm | **$^{87}Sr/^{86}Sr$** | **εNd** |
|---|---|---|---|---|---|---|---|---|
| *Saharan Dust* | | | | | | | | |
| Saharan 1 | 1747 | 5474 | 5355 | 951 | nd | 52 | 0.71865 | nd |
| Saharan 2 | 1918 | 5134 | 5059 | 930 | nd | 49 | 0.71882 | nd |
| *Vegetation Litter* | | | | | | | | |
| Leaves 1 | 30533 | 5987 | 5441 | 1356 | nd | 203 | 0.71019 | nd |
| Leaves 2 | 10237 | 2302 | 1960 | 1857 | nd | 80 | 0.71010 | nd |
| Branches 1 | 14234 | 1315 | 2730 | 581 | nd | 112 | 0.70966 | nd |
| Branches 2 | 12468 | 1122 | 2397 | 504 | nd | 98 | 0.70975 | nd |
| Roots | 16410 | 11390 | 5676 | 2459 | nd | 94 | 0.70976 | nd |
| *Soil*[a] | | | | | | | | |
| GBD2_15 | 306 | 1087 | 1977 | 681 | 8573 | 13 | 0.71293 | -8.39 |
| GBD2_30 | 147 | 643 | 1339 | 404 | 8873 | 9 | 0.71331 | -7.57 |
| GBD2_61 | 45 | 356 | 1189 | 356 | 7913 | 6 | 0.71065 | -2.35 |
| GBD2_91 | 43 | 455 | 1207 | 295 | 6894 | 6 | 0.71064 | -3.66 |
| GBD2_183 | 41 | 174 | 1287 | 444 | 7674 | 4 | 0.70840 | 1.92 |
| GBD2_274 | 28 | 249 | 1043 | 248 | 7374 | 4 | 0.70893 | 0.74 |
| GBD2_305 | 47 | 1026 | 1499 | 353 | 8033 | 12 | 0.71474 | -6.70 |
| GBD2_366 | 35 | 194 | 1068 | 344 | 8153 | 4 | 0.70964 | 1.19 |
| GBD2_427 | 28 | 615 | 1262 | 158 | 10132 | 7 | 0.71496 | -6.54 |
| GBD2_610 | 34 | 326 | 1419 | 264 | 7314 | 4 | 0.71109 | -0.21 |
| GBD2_732 | 36 | 317 | 825 | 160 | 6834 | 2 | 0.70677 | 2.71 |
| GBD2_792 | 43 | 621 | 880 | 278 | 5096 | 4 | 0.71125 | -2.12 |
| GBD2_914 | 29 | 321 | 1196 | 339 | 7074 | 4 | 0.71062 | 0.42 |
| GBD2_1036 | 48 | 258 | 1234 | 347 | 6714 | 4 | 0.70877 | nd |
| GBD2_1097 | 23 | 242 | 946 | 291 | 5995 | 3 | 0.70988 | 2.44 |
| GBD2_1158 | 41 | 215 | 1341 | 324 | 9052 | 2 | 0.70764 | nd |
| GBD2_1219 | 78 | 1276 | 1612 | 277 | 7674 | 12 | 0.71527 | -1.89 |
| GBD2_1250 | 60 | 971 | 1312 | 215 | 8273 | 12 | 0.71508 | -0.97 |
| *Volcanic Rock*[b] | | | | | | | | |
| 04GW12 | 48462 | 7308 | 9060 | 27328 | 5373 | 244 | 0.70388 | 5.45 |
| 00GU44 | 74521 | 5175 | 29483 | 20282 | 5466 | 331 | 0.70380 | 4.34 |
| 03GU75 | 68417 | 4325 | 26106 | 21669 | 5796 | 283 | 0.70385 | 4.67 |

[a] for soil sample names GBD2_X, X=depth in cm

[b] rock samples from Samper et al. (2007).

Table 4: Elemental annual flux ($kg.ha^{-1}.yr^{-1}$), stock ($kg.ha^{-1}$) and residence time (yr) in the Quiock Creek catchment.

| | **Na** | **Ca** | **Mg** | **K** | **Sr** |
|---|---|---|---|---|---|
| **Rainfall flux ($F_{RF}$)** | 83.0 | 11.7 | 11.7 | 6.2 | 0.076 |
| *Sea Salt flux ($F_{SW}$)* | *74.1* | *2.7* | *9.6* | *2.7* | *0.053* |
| *Saharan dust leaching flux ($F_{SD}$)* | *8.9* | *9.0* | *2.1* | *3.5* | *0.023* |
| **Throughfall flux ($F_{TF}$)** | 83.0 | 21.4 | 13.0 | 47.4 | 0.156 |
| *Sea Salt flux ($F_{SW}$)* | *74.1* | *2.7* | *9.6* | *2.7* | *0.053* |
| *Saharan dust leaching flux ($F_{SD}$)* | *8.9* | *9.0* | *2.1* | *3.5* | *0.023* |
| *Leaf excretion flux ($F_{EX}$)* | *0.0* | *9.6* | *1.4* | *41.2* | *0.080* |
| **Vegetation flux ($F_{VEG}$)** | 8.4 | 141.5 | 25.8 | 62.1 | 1.039 |
| *Litter fall flux ($F_{LF}$)* | *8.4* | *131.9* | *24.4* | *20.9* | *0.959* |
| *Leaf excretion flux ($F_{EX}$)* | *0.0* | *9.6* | *1.4* | *41.2* | *0.080* |
| **Vegetation Stock** | 405.1 | 6355.9 | 1180.1 | 1010.6 | 46.3 |
| **Residence time ($T_{res}$)** | 48.2 | 44.9 | 45.7 | 16.0 | 44.6 |
| **Quiock Creek flux ($F_{QC}$)** | 60.9 | 4.5 | 8.0 | 2.2 | 0.051 |

Calculations are described by equations 2 to 9.

Table 1S: ICP AES (for major elements) and ICP MS (for Sr) analyses of rock and vegetation standard reference materials.

| | Al | Ca | Fe | K | Mg | Na | Sr |
|---|---|---|---|---|---|---|---|
| | ppm | ppm | ppm | ppm | ppm | ppm | ppm |
| *Rock standards* | | | | | | | |
| BEN certif[1] | 53312 | 99071 | 89880 | 11534 | 79291 | 23594 | 1370 |
| BEN (this study) | 54289 | 99897 | 90935 | 11739 | 79269 | 23846 | 1655 |
| | 52140 | 95138 | 89888 | 11397 | 76588 | 23325 | |
| GSN certif[1] | 77665 | 17857 | 26250 | 38419 | 13868 | 27971 | 570 |
| GSN (this study) | 77987 | 17562 | 25798 | 35813 | 13629 | 26838 | 531 |
| | 77673 | 17467 | 25594 | 35454 | 13600 | 26723 | 554 |
| | 80519 | 17834 | 26123 | 37214 | 13770 | 27587 | |
| *Vegetation standard* | | | | | | | |
| NIST_SRM 1515 (certif) | 286 | 15260 | 83 | 16000 | 2700 | 24.4 | 25 |
| NIST_SRM 1515 (this study) | 283 | 14441 | 69 | 15216 | 2421 | 55 | |
| | 290 | 14349 | 73 | 15544 | 2478 | 57 | |
| | 283 | 14872 | 75 | 16102 | 2662 | 42 | |
| | 286 | 15014 | 76 | 16307 | 2682 | 42 | |

[1] Recommended values of GSN, BEN are taken from CRPG certificate of analyze (http://helium.crpg.cnrs-nancy.fr/SARM/pages/geostandards.html#).

Table 2S : Sr concentration in throughfall, rainfall and Quiock Creek samples

| Sample name | Date | Sr µmol/l | Sample name | Date | Sr µmol/l | Sample name | Date | Sr µmol/l |
|---|---|---|---|---|---|---|---|---|
| **Throughfall** | | | | | | | | |
| TF col n°1 | 14/11/2011 | 0.136 | TF col n°3 | 25/03/2013 | 0.041 | QC | 16/03/2012 | 0.064 |
| TF col n°2 | 14/11/2011 | 0.129 | TF col n°1 | 27/03/2013 | 0.070 | QC | 04/04/2012 | 0.057 |
| TF col n°1 | 21/11/2011 | 0.025 | TF col n°3 | 27/03/2013 | 0.049 | QC | 09/04/2012 | 0.058 |
| TF col n°2 | 21/11/2011 | 0.121 | TF col n°1 | 29/03/2013 | 0.070 | QC | 13/04/2012 | 0.058 |
| TF col n°3 | 21/11/2011 | 0.038 | TF col n°3 | 29/03/2013 | 0.050 | QC | 19/04/2012 | 0.070 |
| TF col n°1 | 25/11/2011 | 0.035 | TF col n°1 | 01/04/2013 | 0.018 | QC | 23/04/2012 | 0.056 |
| TF col n°2 | 25/11/2011 | 0.026 | TF col n°3 | 01/04/2013 | 0.016 | QC | 26/04/2012 | 0.056 |
| TF col n°3 | 25/11/2011 | 0.035 | TF col n°1 | 03/04/2013 | 0.048 | QC | 08/06/2012 | 0.054 |
| TF col n°1 | 09/04/2012 | 0.012 | TF col n°3 | 03/04/2013 | 0.043 | QC | 03/08/2012 | 0.052 |
| TF col n°2 | 09/04/2012 | 0.067 | TF col n°1 | 25/06/2013 | 0.067 | QC | 05/08/2012 | 0.053 |
| TF col n°3 | 09/04/2012 | 0.037 | TF col n°3 | 25/06/2013 | 0.062 | QC | 10/08/2012 | 0.053 |
| TF col n°1 | 13/04/2012 | 0.126 | TF col n°1 | 26/06/2013 | 0.048 | QC | 16/08/2012 | 0.050 |
| TF col n°2 | 13/04/2012 | 0.076 | TF col n°3 | 26/06/2013 | 0.036 | QC | 07/09/2012 | 0.050 |
| TF col n°3 | 13/04/2012 | 0.049 | TF col n°1 | 28/06/2013 | 0.043 | QC | 05/10/2012 | 0.050 |
| TF col n°2 | 16/04/2012 | 0.027 | | | | QC | 23/10/2012 | 0.049 |
| TF col n°3 | 16/04/2012 | 0.023 | **Rainfall** | | | QC | 26/10/2012 | 0.048 |
| TF col n°1 | 19/04/2012 | 0.119 | RF-MF | 03/08/2012 | 0.039 | QC | 30/11/2012 | 0.037 |
| TF col n°2 | 19/04/2012 | 0.113 | RF-MF | 10/08/2012 | 0.034 | QC | 14/12/2012 | 0.035 |
| TF col n°3 | 19/04/2012 | 0.109 | RF-OVSG | 20/03/2013 | 0.010 | QC | 18/01/2013 | 0.037 |
| TF col n°1 | 23/04/2012 | 0.011 | RF-OVSG | 21/03/2013 | 0.011 | QC | 01/02/2013 | 0.037 |
| TF col n°2 | 23/04/2012 | 0.010 | RF-OVSG | 27/03/2013 | 0.021 | QC | 01/03/2013 | 0.046 |
| TF col n°3 | 23/04/2012 | 0.008 | RF-OVSG | 31/03/2013 | 0.009 | QC | 20/03/2013 | 0.045 |
| TF col n°1 | 05/08/2012 | 0.031 | RF-OVSG | 01/04/2013 | 0.017 | QC | 21/03/2013 | 0.046 |
| TF col n°2 | 05/08/2012 | 0.032 | RF-OVSG | 04/04/2013 | 0.015 | QC | 25/03/2013 | 0.042 |
| TF col n°3 | 05/08/2012 | 0.038 | RF-OVSG | 15/07/2013 | 0.034 | QC | 29/03/2013 | 0.039 |
| TF col n°1 | 10/08/2012 | 0.056 | | | | QC | 01/04/2013 | 0.039 |
| TF col n°2 | 10/08/2012 | 0.060 | **Quiock Creek** | | | QC | 03/04/2013 | 0.042 |
| TF col n°3 | 10/08/2012 | 0.121 | QC | 14/10/2011 | 0.059 | QC | 24/05/2013 | 0.056 |
| TF col n°1 | 16/08/2012 | 0.098 | QC | 10/11/2011 | 0.069 | QC | 21/06/2013 | 0.048 |
| TF col n°2 | 16/08/2012 | 0.115 | QC | 23/11/2011 | 0.068 | QC | 25/06/2013 | 0.051 |
| TF col n°3 | 16/08/2012 | 0.136 | QC | 09/12/2011 | 0.060 | QC | 26/06/2013 | 0.052 |
| TF col n°1 | 21/03/2013 | 0.017 | QC | 06/01/2012 | 0.064 | QC | 28/06/2013 | 0.047 |
| TF col n°3 | 21/03/2013 | 0.015 | QC | 03/02/2012 | 0.061 | QC | 02/07/2013 | 0.049 |
| TF col n°1 | 25/03/2013 | 0.084 | | | | | | |